AD-A049 772 PRINCETON UNIV N J GAS DYNAMICS LAB F/G 20/4
A THREE-DIMENSIONAL STUDY OF FIN-INDUCED SHOCK WAVE TURBULENT B--ETC(U)
JUL 77 D S DOLLING, C D COSAD, S M BOGDONOFF DAAG29-76-G-0269
UNCLASSIFIED ARO-14026.1-EX NL

| OF |
AD A049772

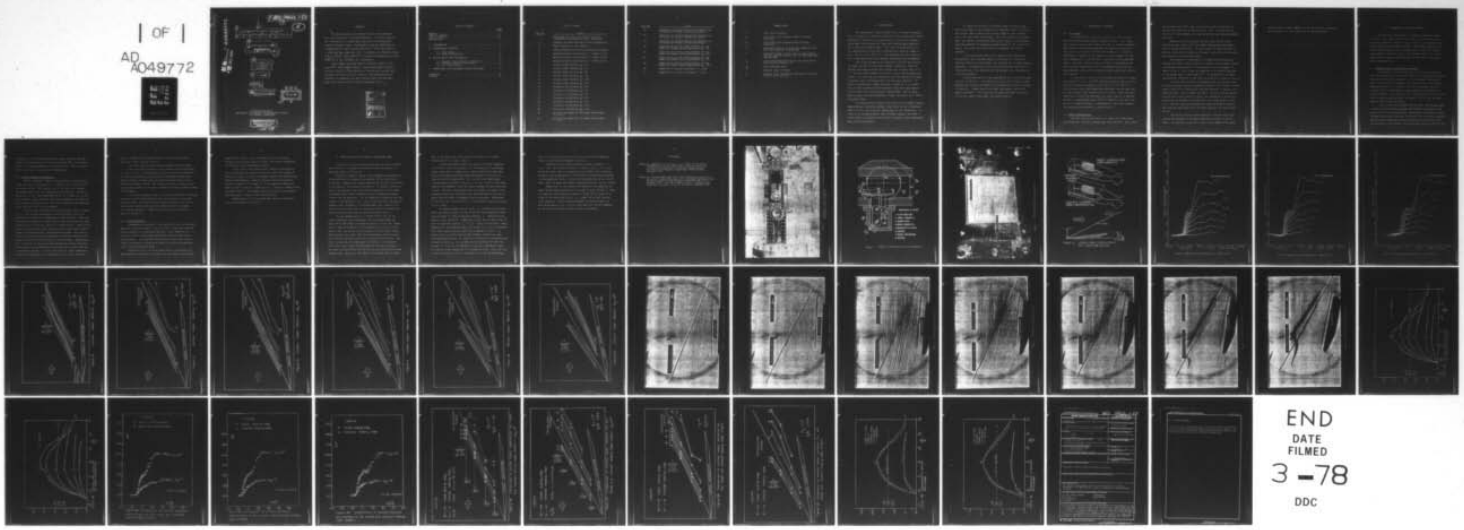

END
DATE FILMED
3-78
DDC

AD A049772
AD No.
DDC FILE COPY

(18) ARO 14026.1-EX

(19)

(5)

(6) A THREE-DIMENSIONAL STUDY OF FIN-INDUCED SHOCK WAVE TURBULENT BOUNDARY LAYER INTERACTION

(9) INTERIM TECHNICAL REPORT.

For the Period

15 June (76) — 15 June (77)

(10) D. S. Dolling
C. D. Cosad
S. M. Bogdonoff
I. E. Vas

(11) 15 July (77)

(12) 52p.

U. S. ARMY RESEARCH OFFICE

(13) GRANT DAAG29-76-G-0269

DDC
RECEIVED
FEB 10 1978
B

PRINCETON UNIVERSITY
DEPARTMENT OF AEROSPACE AND MECHANICAL SCIENCES
GAS DYNAMICS LABORATORY

DISTRIBUTION STATEMENT A
Approved for public release;
Distribution Unlimited

145 770

ABSTRACT

Surface pressure distributions and oil streak patterns have been measured in the three-dimensional flowfield caused by the interaction of a skewed shock wave with a two-dimensional turbulent boundary layer. The boundary layer was developing on a 45° sweptback, sharp leading edged plate. Tests were made at a freestream Mach number of 2.95, a freestream unit Reynolds number of 6.3×10^7/m (1.6×10^6/in), a stagnation temperature of about 265°K and at near adiabatic wall temperature.

Measurements have been made for generator angles in the range 0° to 12° in 2° increments. These measurements represent the first phase of a study which will include heat transfer measurements and details of the flowfield. The measured data are presented and compared with data obtained under the same shock wave conditions but with a different boundary layer.

ACCESSION for
NTIS White Section
DDC Buff Section
UNANNOUNCED
JUSTIFICATION
BY
DISTRIBUTION/AVAILABILITY CODES
Dist. AVAIL. and/or SPECIAL

TABLE OF CONTENTS

LIST OF FIGURES

NOMENCLATURE

P	local static pressure
P_1	calculated static pressure ahead of oblique shock wave
P_2	calculated static pressure behind oblique shock wave
X	coordinate parallel to tunnel axis measured from the shock generator leading edge
Y	coordinate normal to the X axis in the plane of the test surface measured from the shock generator leading edge.
X_s	X coordinate measured from the calculated shock wave location (see Fig. 4).
α_G	shock generator angle
δ	boundary layer thickness
δ_1	boundary layer thickness at beginning of pressure rise for given value of Y .

I. INTRODUCTION

The experimental study reported briefly on herein represents the first phase of a detailed investigation being made of the three-dimensional flowfield of a viscous-inviscid interaction between a shock wave, from a sharp, 45° swept back leading edged generator, and a turbulent boundary layer. This study is being carried out at a Mach number of 2.95 and a freestream unit Reynolds number of 6.3×10^7 m^{-1} (1.6×10^6 in^{-1}). Data obtained from this study will aid in the modelling of this complex three-dimensional phenomenon.

The current program is an extension of earlier work carried out under contract to the Flight Dynamics Laboratory. Detailed studies were made using the thick tunnel wall boundary layer (i.e., δ = .55") at a Mach number of 2.95 with a sharp leading edged generator. For this case the interaction could be studied up to about 8 boundary layer thicknesses away from the shock generator. To obtain a considerably "larger picture" in terms of δ a further set of tests was made using the boundary layer which developed on a flat plate with a sharp straight leading edge. Both of these test programs have been documented in detail by Oskam et al (1975) and Oskam (1976).

This second study, using a flat plate with an unswept leading edge, produced a turbulent boundary layer which varied in thickness from 0.11" to 0.18" along the leading edge of the interaction. In terms of an average boundary layer thickness however, the interaction could be studied at up to about 30 boundary layer thicknesses away from the generator.

To reduce the variation of boundary layer thickness along the leading edge of the interaction, an important factor in scaling, the unswept leading edge of the original study has been replaced with a 45° swept back leading edge. With this geometrical arrangement, the surface flow patterns and surface pressure distributions have been measured for generator angles from 2° to 12° in 2° increments. This study constitutes the first phase of the present contract.

It was anticipated that, with a swept leading edge plate, the boundary layer thickness ahead of and along the interaction direction would vary considerably less than for the straight leading edge model. A comparison of the two sets of results would aid in the evaluation of the importance of the boundary layer thickness as a scaling parameter.

A brief description of the experimental facility and the model is given in Section 2. The measured pressure distributions, isobar patterns and surface flow angles are presented and briefly discussed in Section 3. Comparisons of the swept and unswept results are made in Section 4. This brief interim report provides an outline of the work done to date under the present contract.

2. EXPERIMENTAL EQUIPMENT

2.1 Wind tunnel

The experimental study was carried out in the Princeton University high Reynolds number supersonic tunnel. This tunnel has a working section 20cm x 20cm (8" x 8"), a nominal freestream Mach number of 3 and may be operated at stagnation pressures in the range 4×10^5 to 34×10^5 Nm^{-2} (60 to 500 psi). Since the compressed air supply for the tunnel is stored outdoors the flow total temperature is variable but is typically in the range 260-270°K. The actual value at any given time is determined by the local external temperature, the Joule-Thompson drop across the main regulator valve, and the amount of heat transferred from the inlet piping.

In the current study all of the tests were made at a stagnation pressure of 6.8×10^5 Nm^{-2} (100 psi) corresponding to a freestream unit Reynolds number of 6.3×10^7 m^{-1} (1.6×10^6 in^{-1}). With the above mentioned temperature considerations the model was at near adiabatic wall conditions for all tests. Under the above conditions and with the compressed air supply tanks at a maximum pressure of approximately 20×10^6 Nm^{-2} (3000 psi) the tunnel can be run for about 6 minutes. A photograph of the tunnel showing the nozzle and test section is given in Fig. 1.

2.2 Model configurations

The test surface consisted of a 1.27cm (.5") thick brass flat plate with the sharp leading edge swept back 45°. This plate,

approximately 67cm (24") long, spanned the tunnel horizontally and was mounted 5.08cm (2") above the tunnel floor. To avoid any possibility of flow blockage, the lower tunnel wall was recessed beneath the plate.

Mounted vertically between the test plate and the tunnel ceiling was the 1.27cm (.5") thick sharp leading edge shock generator of length 25.4cm (10"). To avoid leaks, the edges adjacent to the test plate and the tunnel ceiling were lined with nylon to ensure good sealing at any generator angle.

The generator is supported by a streamlined arm projecting through the tunnel side wall which is linked to a drive wheel through a calibrated screw system. A line drawing of this arrangement is shown in Fig. 2. This allows the generator to be manually adjusted to any chosen angle in the range 0-12°. A photograph of the model configuration installed in the tunnel test section is shown in Fig. 3.

The flat test plate was instrumented with four parallel rows of static pressure orifices located at 2.92cm (1.15"), 5.46cm (2.15"), 8.64cm (3.4") and 11.18cm (4.4") from the generator in the zero incidence position. Each of these rows had 47 orifices with the spacing varying from .127cm (.05") to 1.27cm (.5") depending on the anticipated position through the interaction. This large number of taps (i.e., 188) was required to ensure that complete detailed pressure distributions were obtained in the shock generator incidence range 0°-12°.

The surface pressures were sampled by a 48 port Model 48J4 scanivalve connected to the model tappings via a bank of plastic tubes. The pressure levels were sensed using a DRUCK strain gauge

type transducer, (Model PDCR22), digitized and then processed by an IBM System 7 on line directly to an IBM 158 machine.

3. DISCUSSION OF DATA AND ANALYSIS

The coordinate system used in presenting the data is shown in Fig. 4. Data taken along pressure tap rows parallel to the X axis are presented in terms of X_s/δ_I where X_s is measured relative to the calculated shock location. This enables data for different shock strengths to be compared since it takes into account the movement of the shock itself with generator angle. δ_I corresponds to the boundary layer thickness at the start of the interaction pressure rise.

3.1 Boundary layer entering the interaction

As mentioned in the introduction the thickness of the boundary layer entering the interaction tends to increase with increasing distance from the shock generator. For the unswept leading edge model, the variation in boundary layer thickness from the inboard pressure tap row at Y = 2.92cm (1.15") to the outboard row at Y = 11.18cm (4.4") is about 66% at a shock generator incidence of 2° and about 44% at an incidence of 12°. The decrease in this variation with increasing shock generator incidence is due to the increased angle of the interaction region.

In the current test program with the swept leading edge model, a series of pitot surveys was made to determine the boundary layer growth over the new configuration. Measurements were made at several streamwise positions along each of the four rows of pressure tappings. Coupling these measurements with the pressure distributions gives the variation of the boundary layer thickness along the start of the

interaction. The variation in boundary layer thickness from the inboard to outboard pressure tap rows was about 50% at a generator angle of 2° and about 20% at an incidence of 12°. This is significantly less than for the original configuration.

3.2 Surface pressure distributions

Figures 5 through 7 show the surface pressure distributions along tap rows corresponding to Y = 2.92cm (1.15"), 5.46cm (2.15") and 8.64cm (3.4"). The pressure axis is the local wall pressure non-dimensionalized by the freestream static pressure. The horizontal axis is X_s non-dimensionalized by δ_1, where δ_1 is the local boundary layer thickness immediately upstream of the start of the interaction pressure rise. Each figure shows data for generator angles from 0° to 12° in 2° increments.

It can be seen immediately from these figures that, in terms of δ_1, the upstream propagation of the disturbance due to the shock wave is essentially independent of shock strength. Typically the upstream propagation is about $12\delta_1$ for the two inboard tap rows increasing to a little over $13\delta_1$ at Y = 8.64cm (3.4"). These conclusions are identical to those found earlier by Oskam (1976) using an unswept leading edge plate. As emphasized by Oskam, this finding is quite different from two-dimensional interactions where the upstream effect is a strong function of shock strength. Depending on the Y position of the tap row and the generator angle, the downstream extent of the interaction, measured from the shock location is between 20 and 40δ. It can be seen that the larger interaction lengths are associated with low generator angles and vice-versa.

This is brought out most clearly for the pressure distributions along the inboard tap row (Fig. 5).

The static pressure distributions obtained along the rows Y = constant have been plotted as isobar patterns and are presented in Figs. 8 to 13. The pressures P_1 and P_2 are the static pressures in front of and behind the calculated oblique shock respectively. Shock strength and shock angle have been calculated using a free-stream Mach number of 2.95. The pressure difference between P_1 and P_2 has been divided into 10 equal increments and these isobars plotted on the figures.

For a given generator angle it can be seen that with increasing distance from the shock generator the isobars tend to spread away from the shock. As noted by Oskam (1976) the pattern does not display conical symmetry but does tend toward cylindrical symmetry far from the generator. Comparisons with previous studies are given in Section 4.

3.3 Oil flow patterns

Photographs of surface oil flow patterns for all of the shock generator angles are shown in Figs. 14 to 20. These were obtained using a mixture of a fluorescent dye and a light commercial oil. A very thin film of this mixture was painted on the surface of the pressure plate and illuminated with an ultra-violet lamp. Once a steady flow pattern had been established at a particular generator angle, the photograph was taken.

Reference to Fig. 14, which shows the oil flow pattern at a shock generator incidence of 0° shows that the sweep of the leading

edge does not result in any flow angularity at the surface. Throughout the entire region of interest the surface streamlines are parallel to the freestream direction.

These surface flow patterns were reduced to quantitative data by measuring the angles of local oil lines with respect to the X-axis along a line of Y = constant (which coincides with the pressure measurements). Results obtained from that process at generator angles of 2° through 12° in two degree increments are shown in Figs. 21 and 22. These are at Y values of 5.46cm (2.15") and 8.64cm (3.4"). The computed shock wave angle for each shock generator angle is shown on the left-hand axis.

Comparisons of the flow angles with those of the earlier study are discussed in Section 4.

4. COMPARISONS WITH THE UNSWEPT LEADING EDGE MODEL

Figures 23, 24, and 25 show comparisons of surface pressure distributions on the swept and unswept leading edge models for generator angles of 4° and 10°.

Plotted in terms of X_s/δ_1 both the swept and unswept distributions tend to collapse on one another for any given set of conditions. Sweeping the leading edge back by 45° has little effect on the shape of the pressure distribution. In terms of the thickness of the boundary layer entering the interaction in the swept and unswept models the difference naturally becomes more marked further from the generator. For the comparisons along the two rows closest to the generator (i.e., Figs. 23 and 24) the difference in boundary layer thickness is at maximum about 15%. Clearly, differences of this order have no significant effects on either the pressure distribution shape or absolute pressure levels.

For the comparisons at Y = 8.64cm (3.4"), Fig. 25, the entering boundary layer thicknesses for the unswept model are about 15% to 20% higher at generator angles of 4° and 10°, respectively. Small differences in the pressure distributions can be seen at 10°. During the initial pressure rise the swept leading edge pressures are higher than the corresponding unswept values. Just ahead of the shock location, a cross-over point occurs. The trend is reversed and becomes more noticeable. In the typical "dip" which occurs about $5\delta_1$ downstream of the shock location, the swept leading pressure are several per cent below those of the unswept case. Basically, the shapes of the curves stay the same

but, in the swept case, the pressure distribution is slightly "stretched" on the X_s/δ_1 scale.

To more completely assess the effects of the 45° sweepback on the whole interaction region (i.e., extending out from the generator about 30δ), a comparison of isobar patterns has been made. These are presented for shock generator angles of 4° and 10° in Figs. 26 and 27, respectively. For clarity, only those isobars corresponding to pressure rises of .2, .4, .6, .8 and 1.0 are shown. Ahead of the shockwave little difference between the two conditions is seen. The small differences which are present, as noted in the pressure plots, occur along the outer tap rows where it was anticipated that the effect of sweepback would be greatest. Downstream of the shock wave the differences in the patterns become more marked, but not large.

To examine whether or not X_s/δ_1 is a suitable scaling parameter the isobar patterns for the 4° and 10° shock generator angles are also shown in terms of absolute distance, X . These plots are shown in Figs. 28 and 29. Comparison of Fig. 26 with 28 and Fig. 27 with 29 shows that scaling X_s by δ_1 reveals no consistent trends. Depending on the generator angle and the particular tap row examined, the isobar patterns may be either drawn together or apart. For several sets of points along the two outboard pressure tap rows, non-dimensionalizing by δ_1 results in a measure of overcompensation. It could be that δ_1 is a primary scaling parameter but that the correct δ to use is not necessarily the value immediately ahead of a point in the interaction in a streamwise sense. Since the flow is not constrained in the Y direction, as in the two-dimensional

case, it may not be strictly correct to try and scale properties along the undisturbed streamwise direction.

Comparison of the isobar patterns plotted in terms of X (i.e., Figs. 28 and 29) with those in terms of X_s/δ_1 (i.e., Figs. 26 and 27) shows that the spreading of the isobars with increasing distance from the generator is not noticeably altered when presented in non-dimensional terms. This can be seen most clearly for the 10° data. Both the swept and unswept measurements exhibit similar trends.

Comparisons of the surface flow angles for the swept and unswept leading edge configurations are shown in Figs. 30 and 31. Data are shown for shock generator angles of 4° and 10° at values of Y = 5.4cm (2.15") and 8.64cm (3.4"), i.e., about 14δ and 24δ from the shock generator. The differences between the data are small and with an accuracy of $\pm$1°, it can be concluded that the 45° sweepback has no significant effect on the surface flow pattern.

REFERENCES

Oskam, B., Bogdonoff, S. M., Vas, I. E., "Study of the Three-Dimensional Flow Field Generated by the Interaction of a Skewed Shock Wave with a Turbulent Boundary Layer". Air Force Flight Dynamics Laboratory, AFFDL-TR-75-21, February 1975.

Oskam, B., "Three-Dimensional Flow Fields Generated by the Interaction of a Swept Shock Wave with a Turbulent Boundary Layer". Princeton University Gas Dynamics Laboratory Rept. 1313, December 1976. Also Ph.D. Thesis, Dept. of Aerospace and Mechanical Sciences, Princeton University, December 1976.

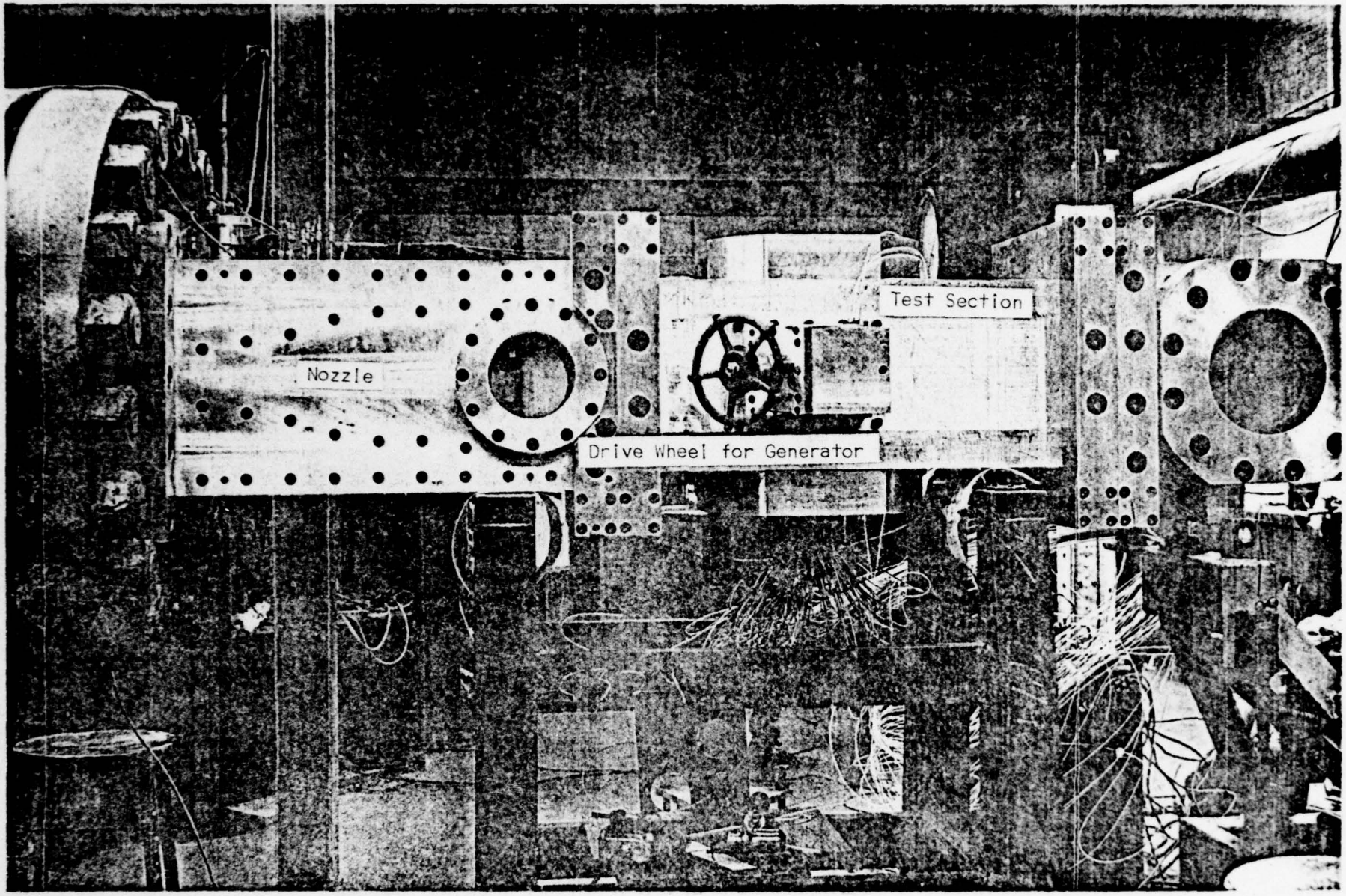

Figure 1 Photograph of Tunnel with Section for Three-Dimensional Shock Boundary Layer Interaction

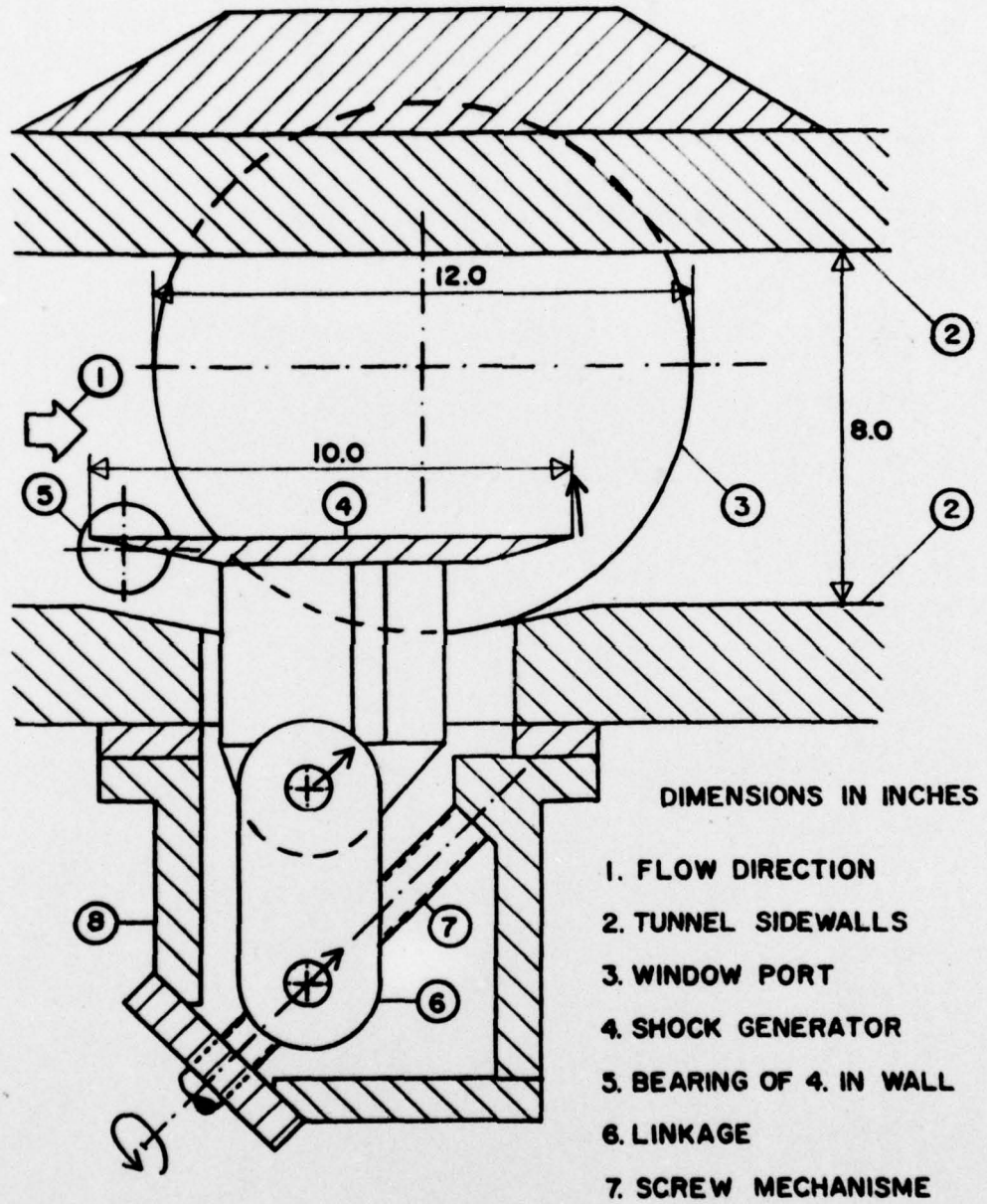

Figure 2 | Schematic of Shock Generator and Drive Mechanism

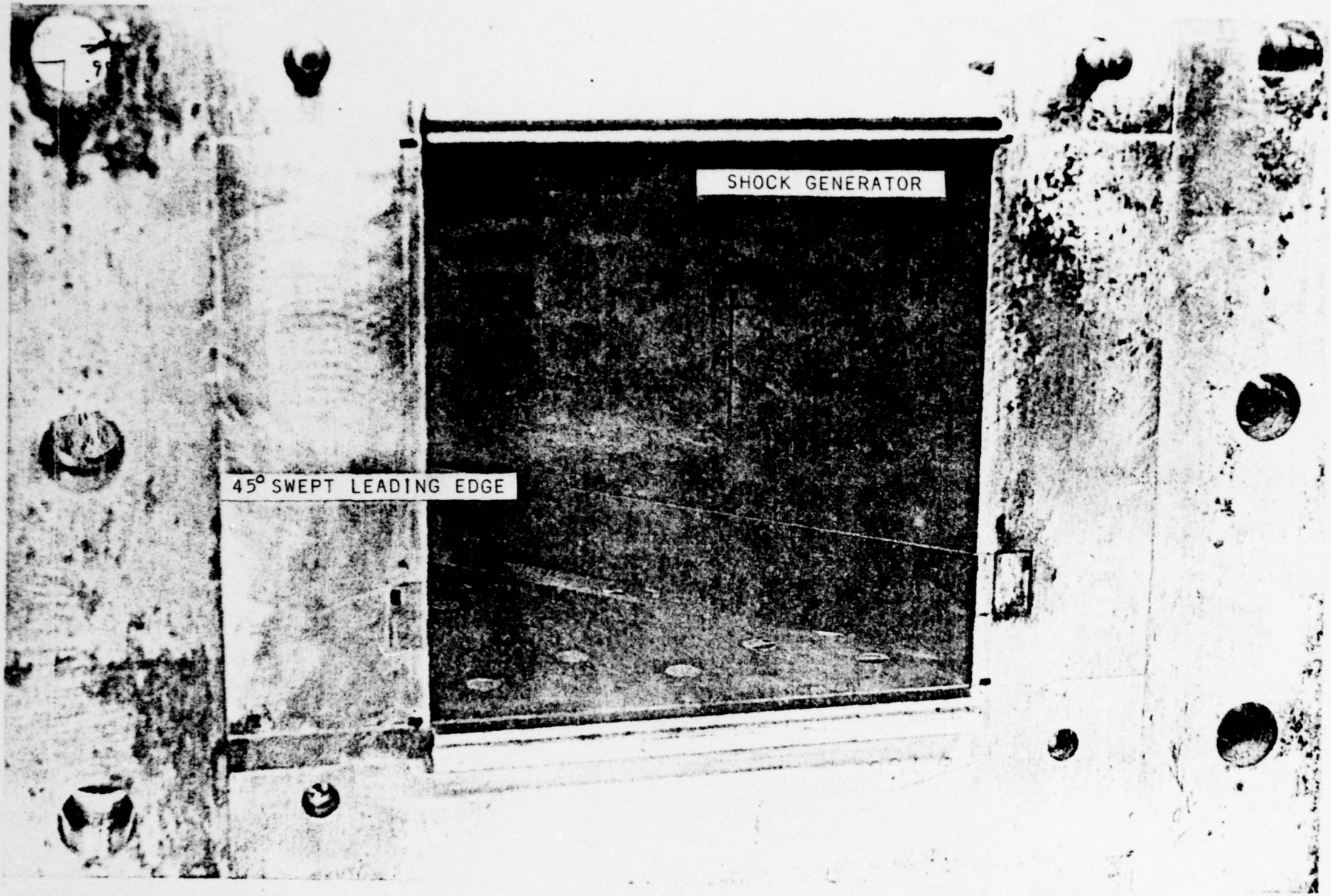

Figure 3 Model installed in test section

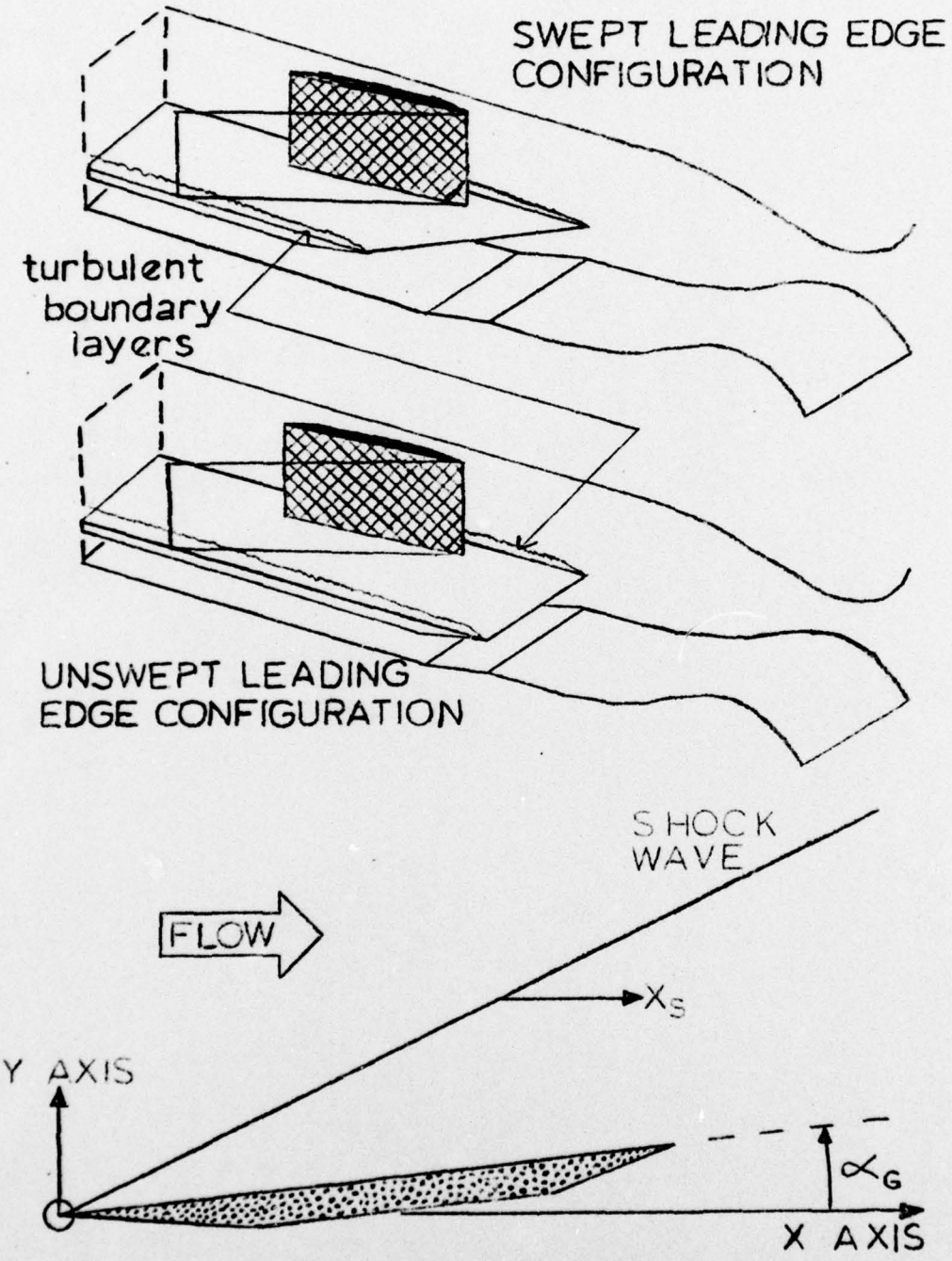

Figure 4 Leading edge configurations and coordinate system

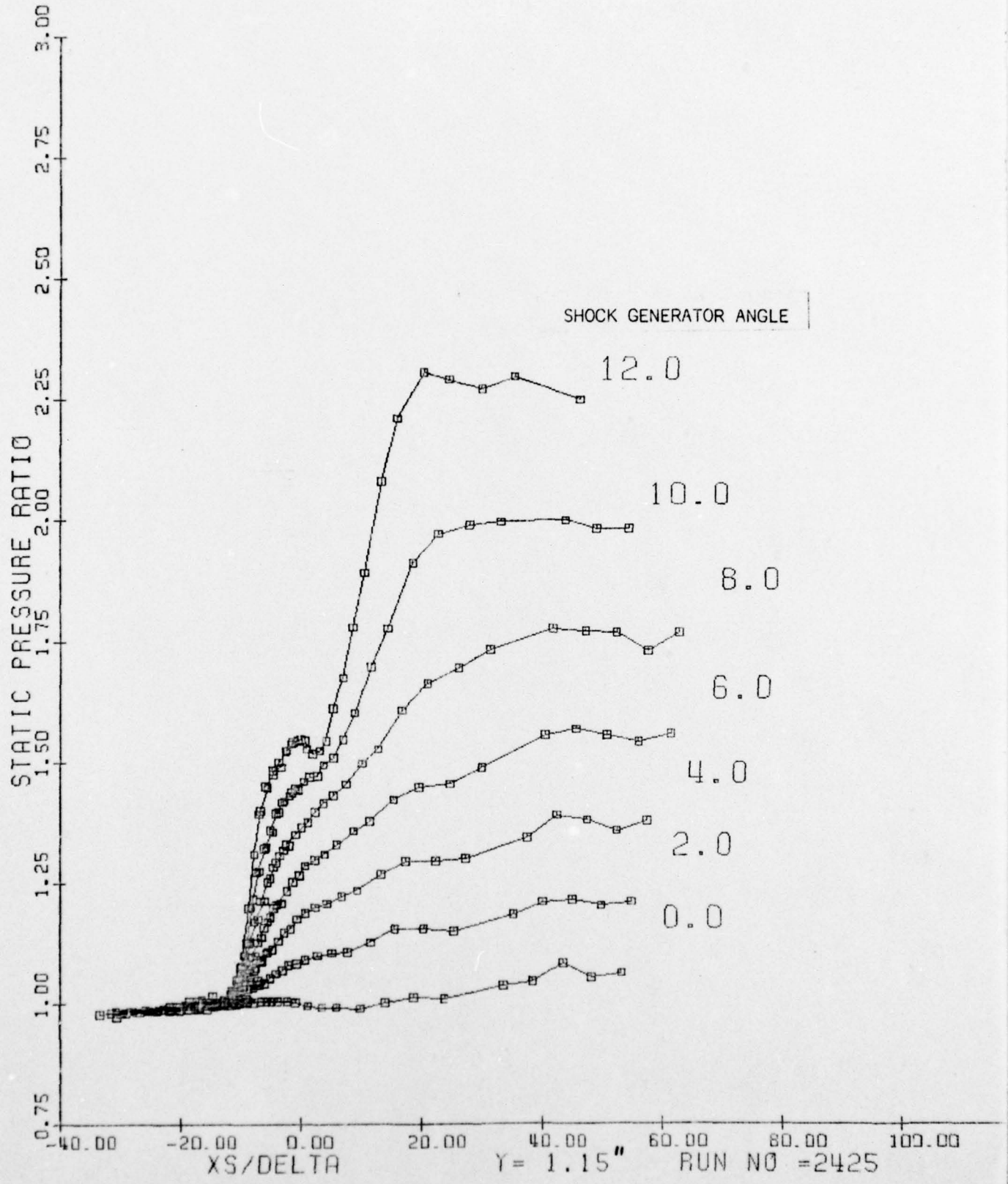

Figure 5 Measured Pressure Distribution Y = 2.92cm (1.15")

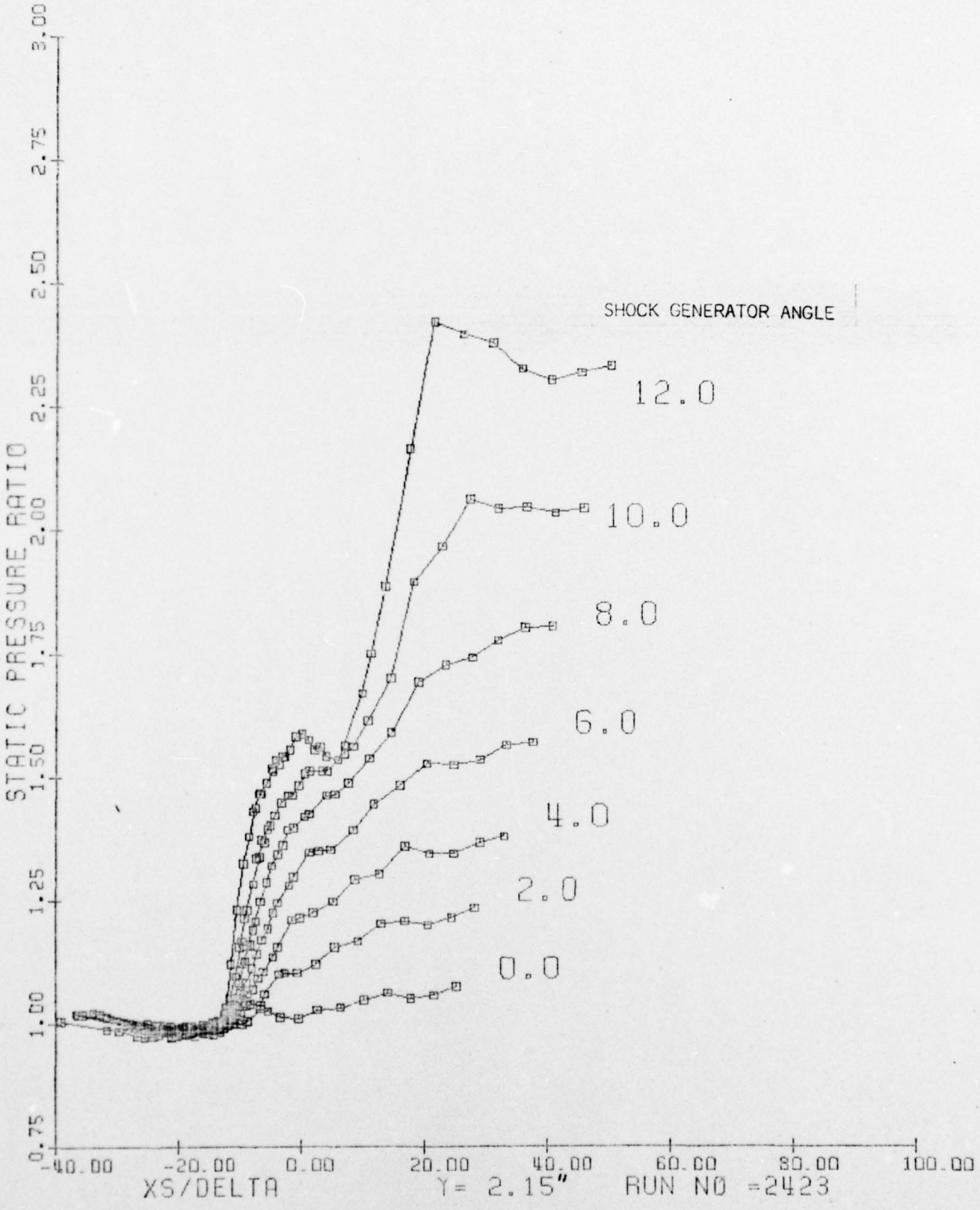

Figure 6 Measured Pressure Distribution Y = 5.46cm (2.15")

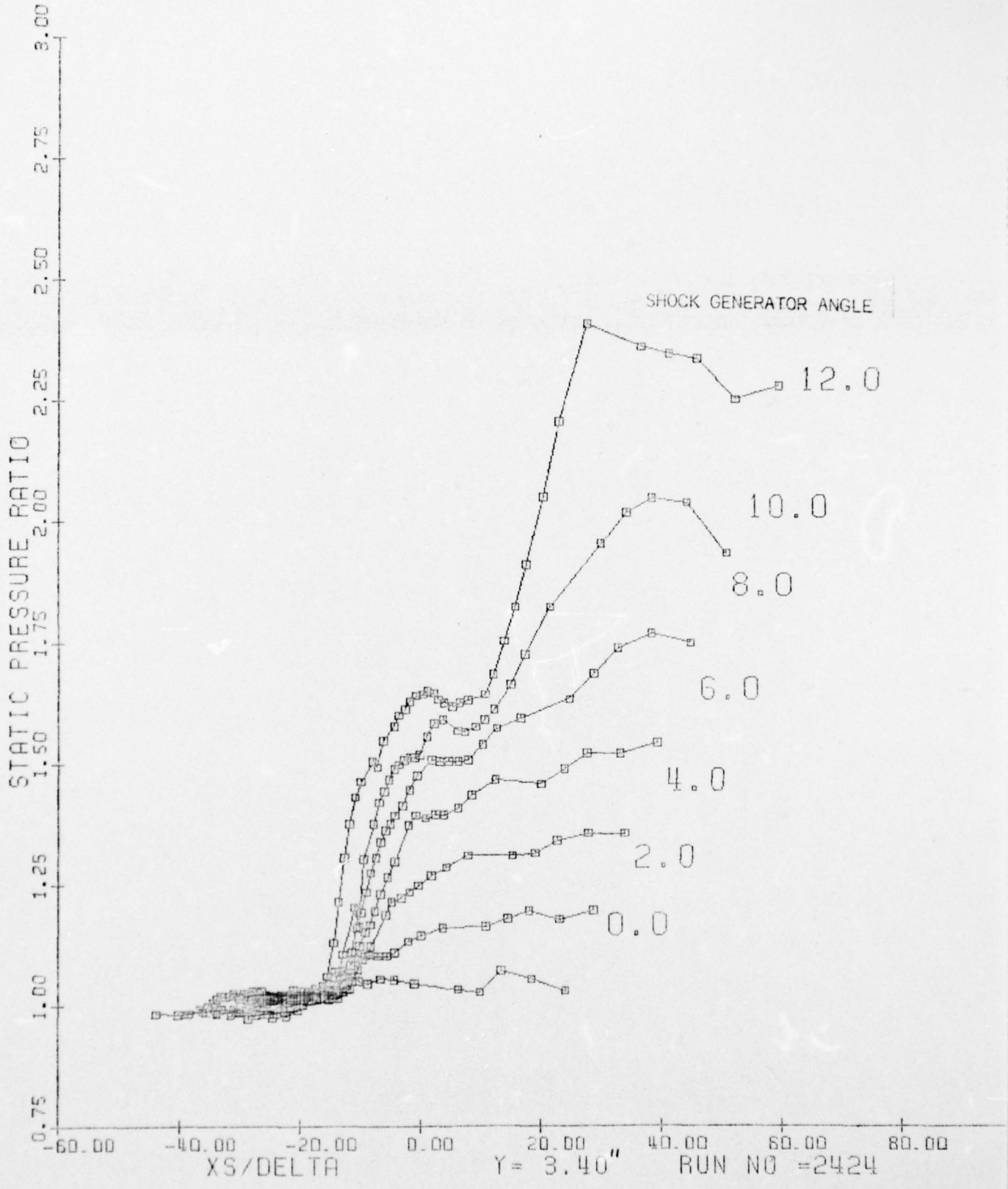

Figure 7 Measured Pressure Distribution Y = 8.64cm (3.4")

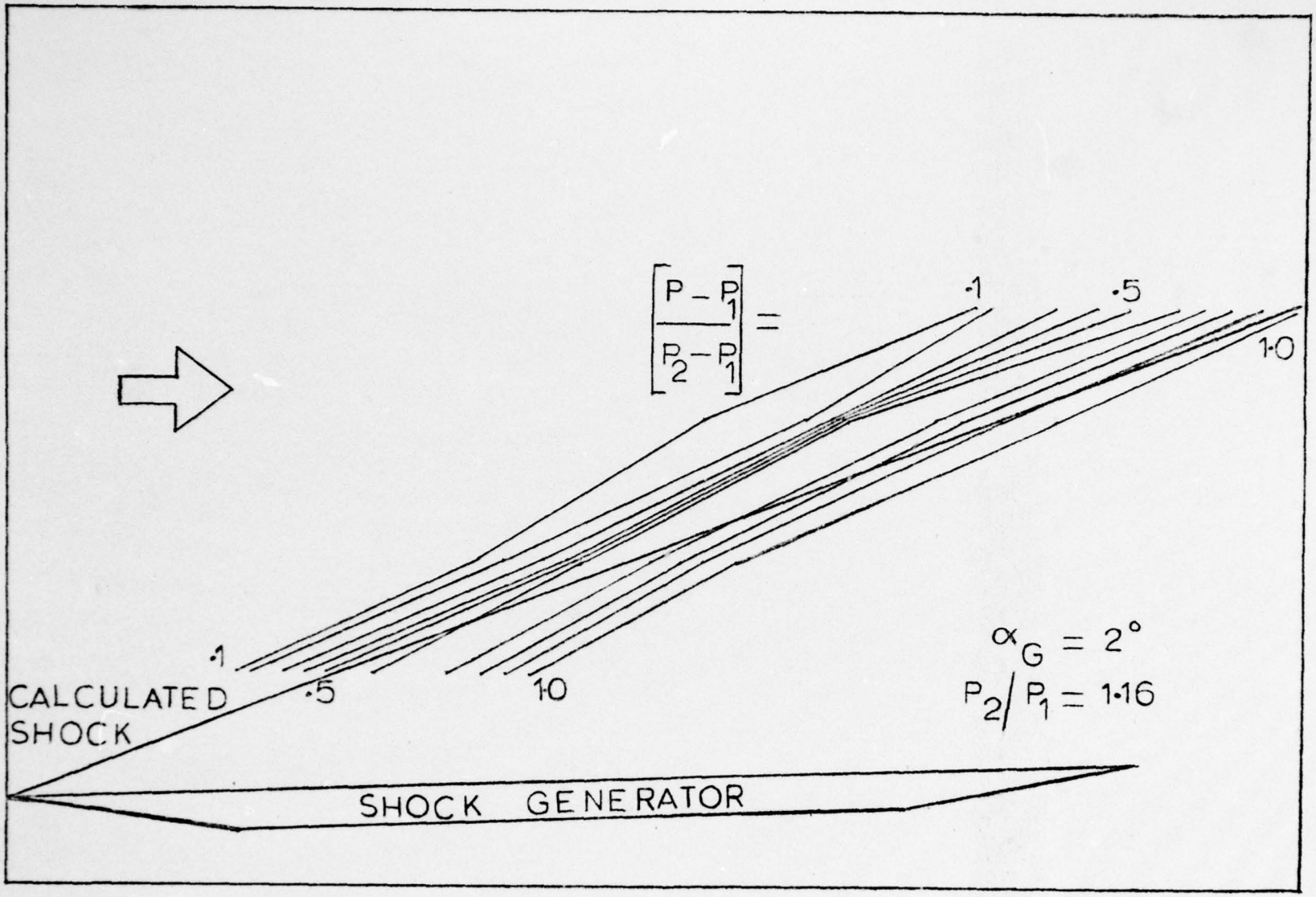

Figure 8 Surface Isobar Patterns $\alpha_G = 2°$

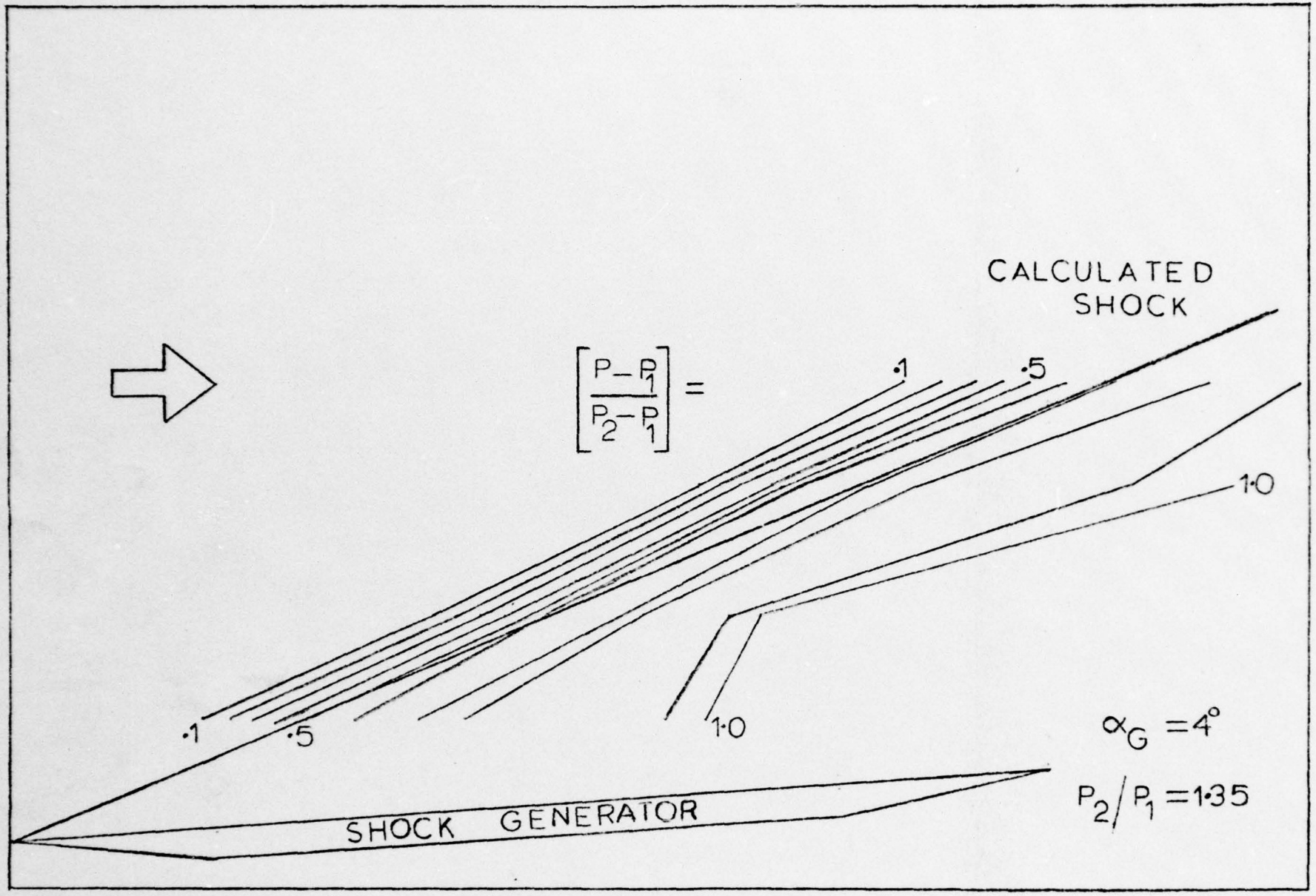

Figure 9 Surface Isobar Patterns $\alpha_G = 4°$

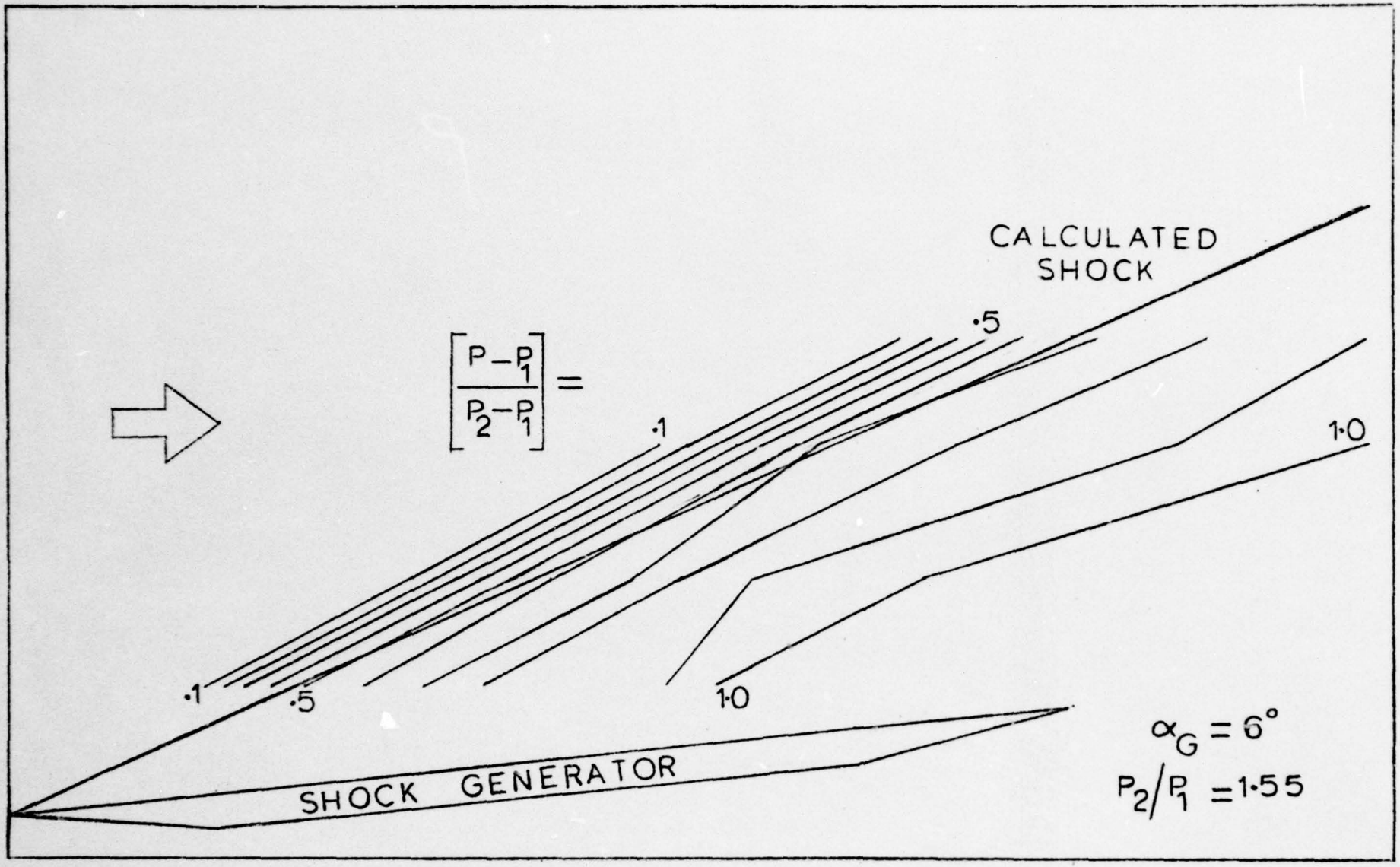

Figure 10 Surface Isobar Patterns $\alpha_G = 6°$

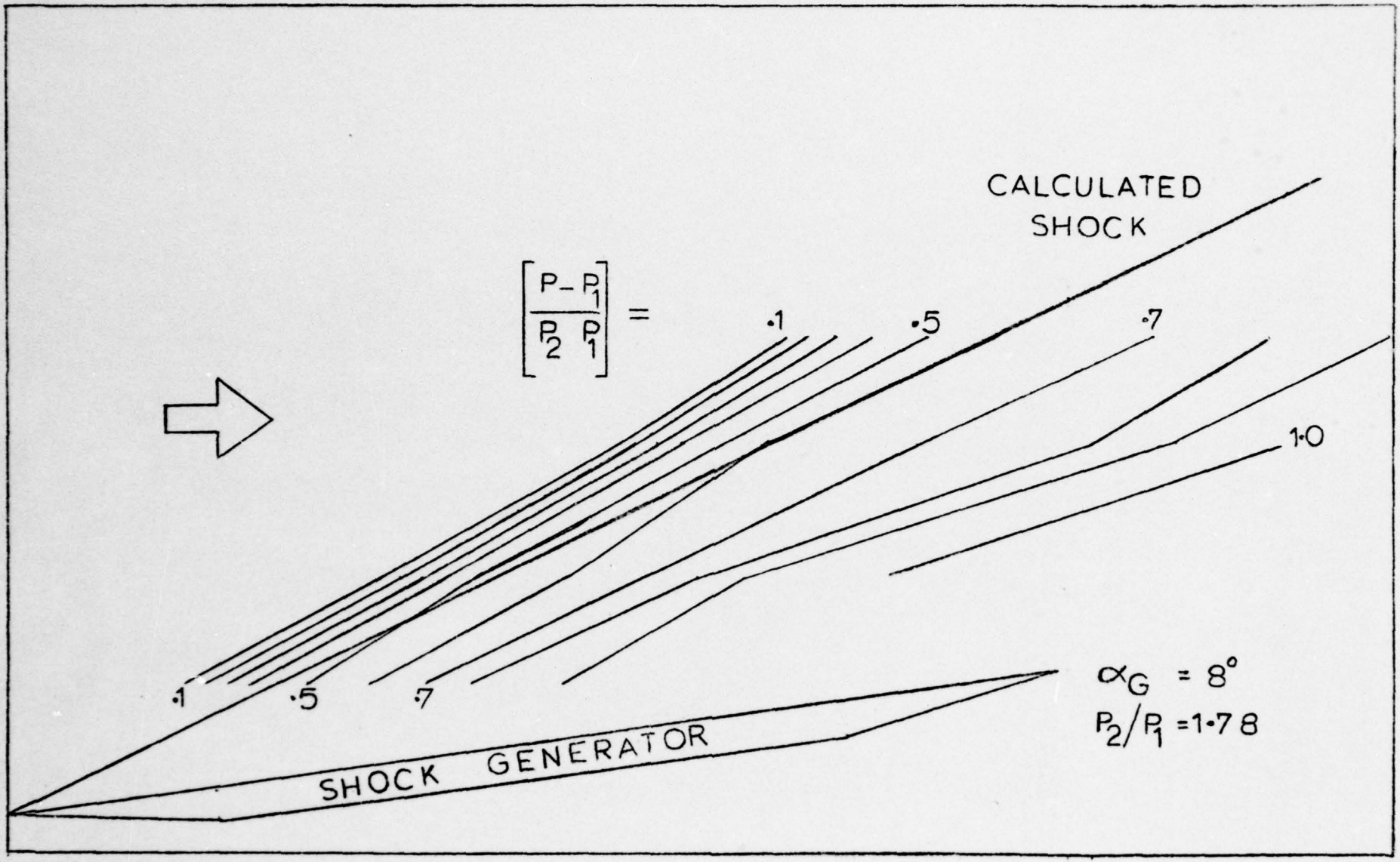

Figure 11 Surface Isobar Patterns $\alpha_G = 8°$

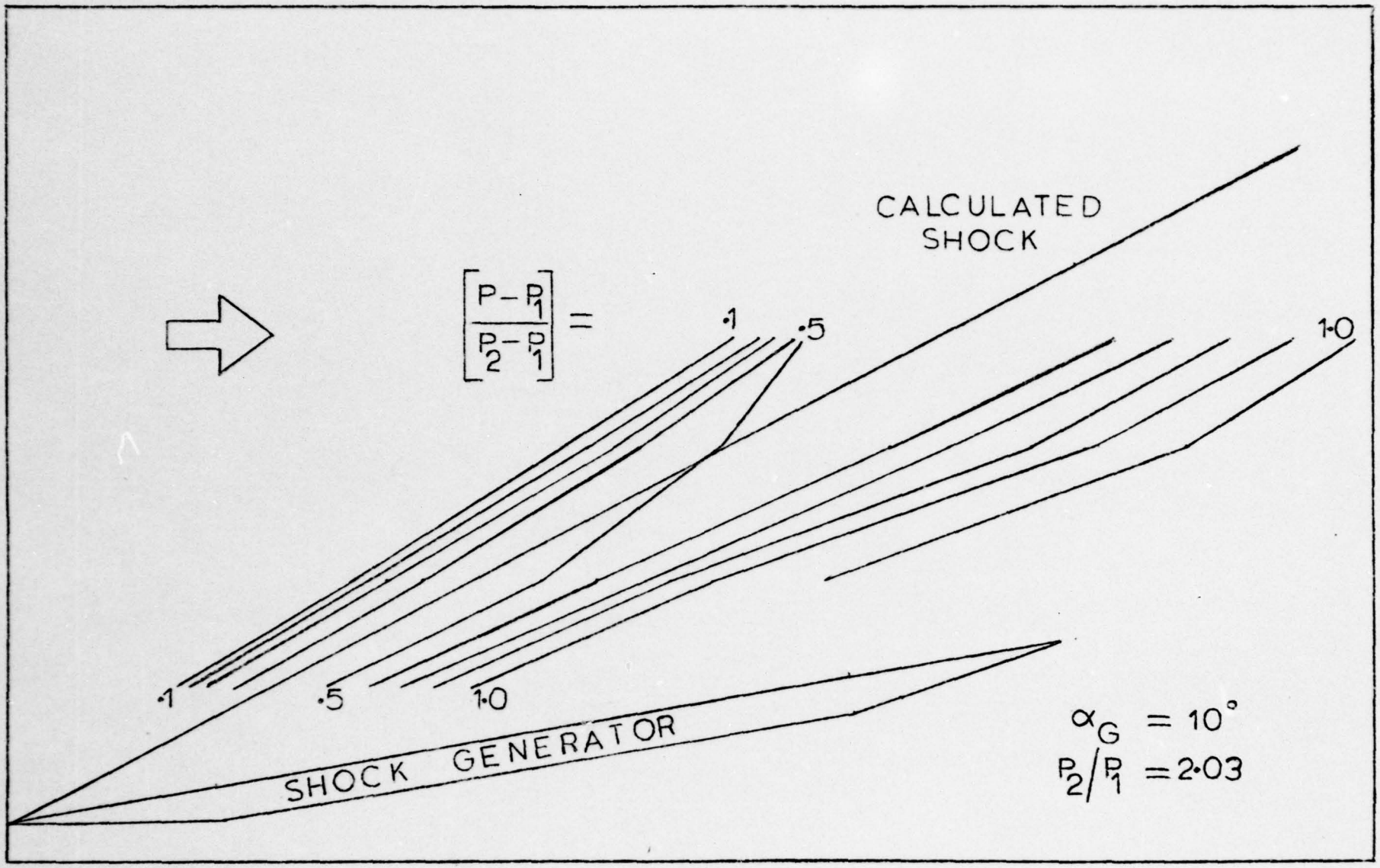

Figure 12 Surface Isobar Patterns α_G =10°

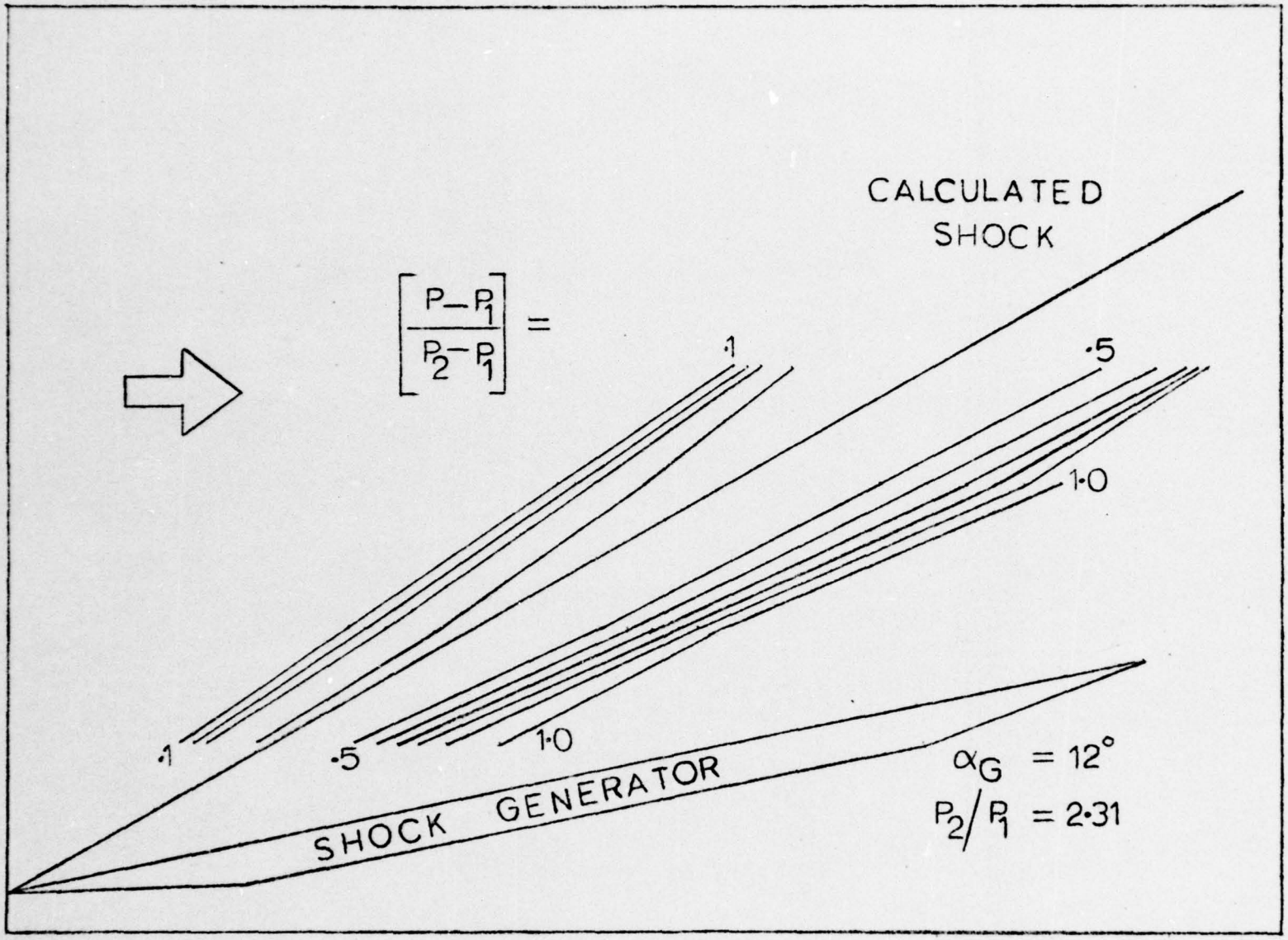

Figure 13 Surface Isobar Patterns $\alpha_G = 12°$

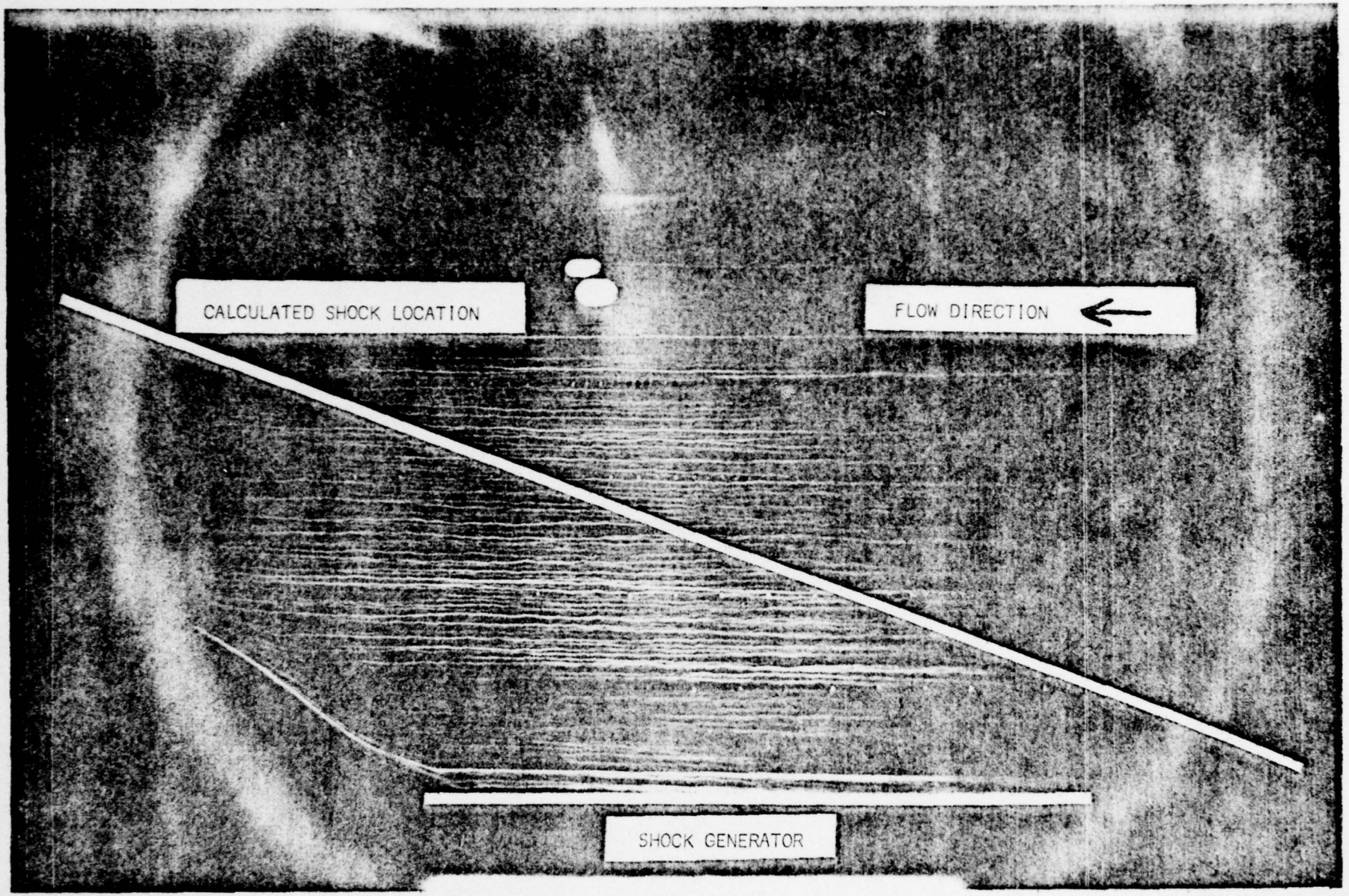

Figure 14 Surface Oil Flow Patterns $\alpha_G = 0°$

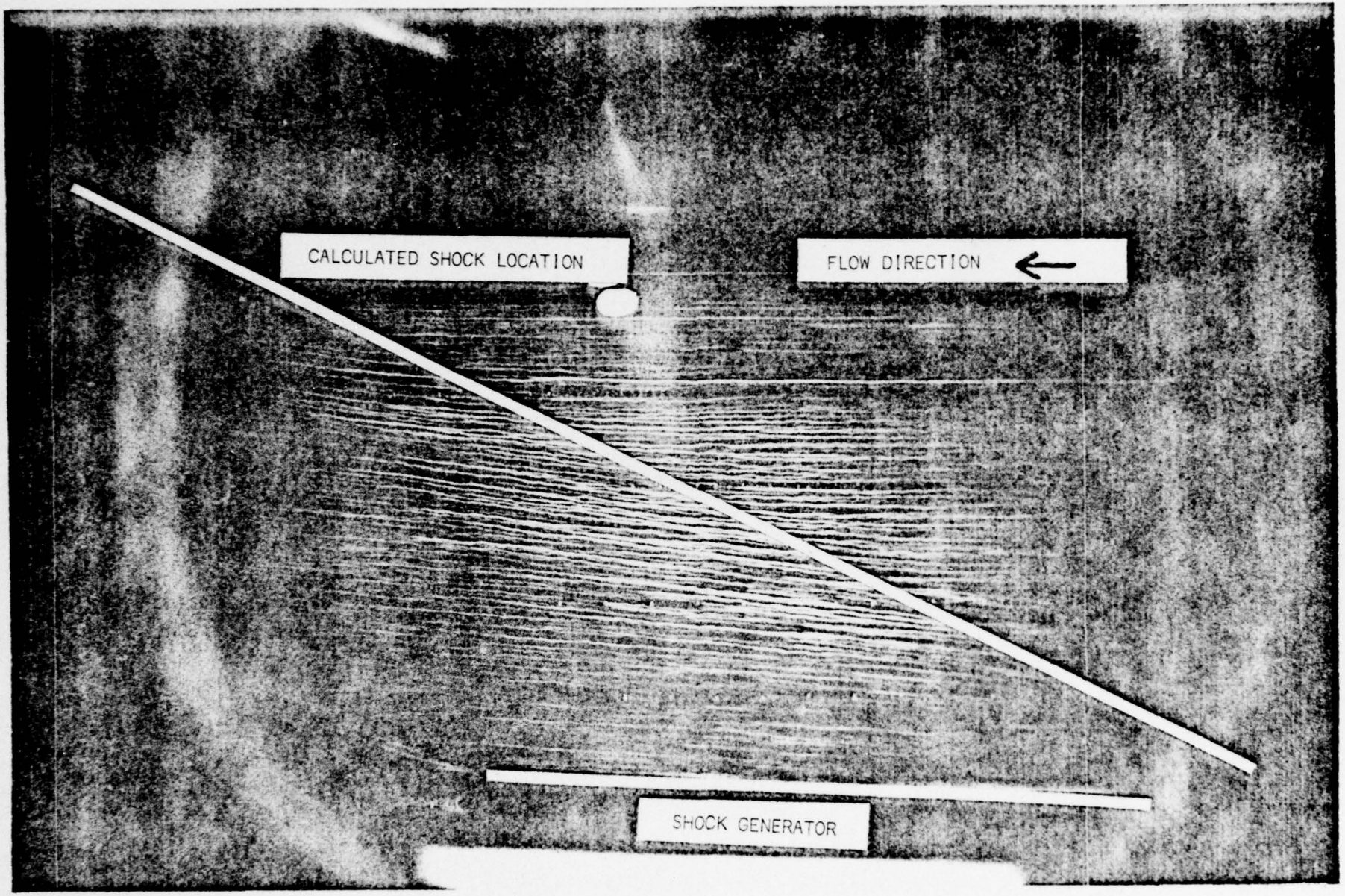

Figure 15 Surface Oil Flow Patterns $\alpha_G = 2°$

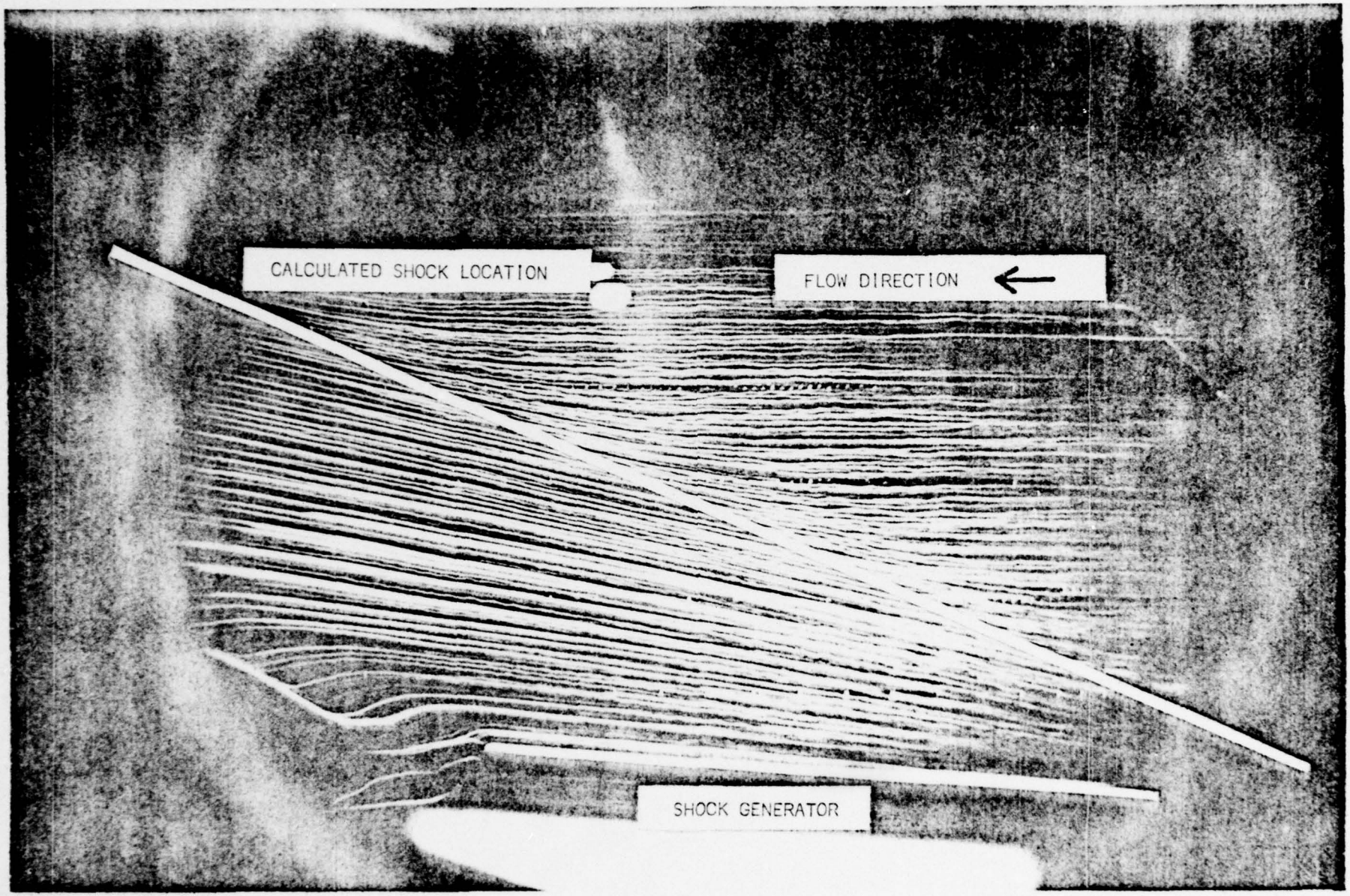

Figure 16 Surface Oil Flow Patterns $\alpha_G = 4°$

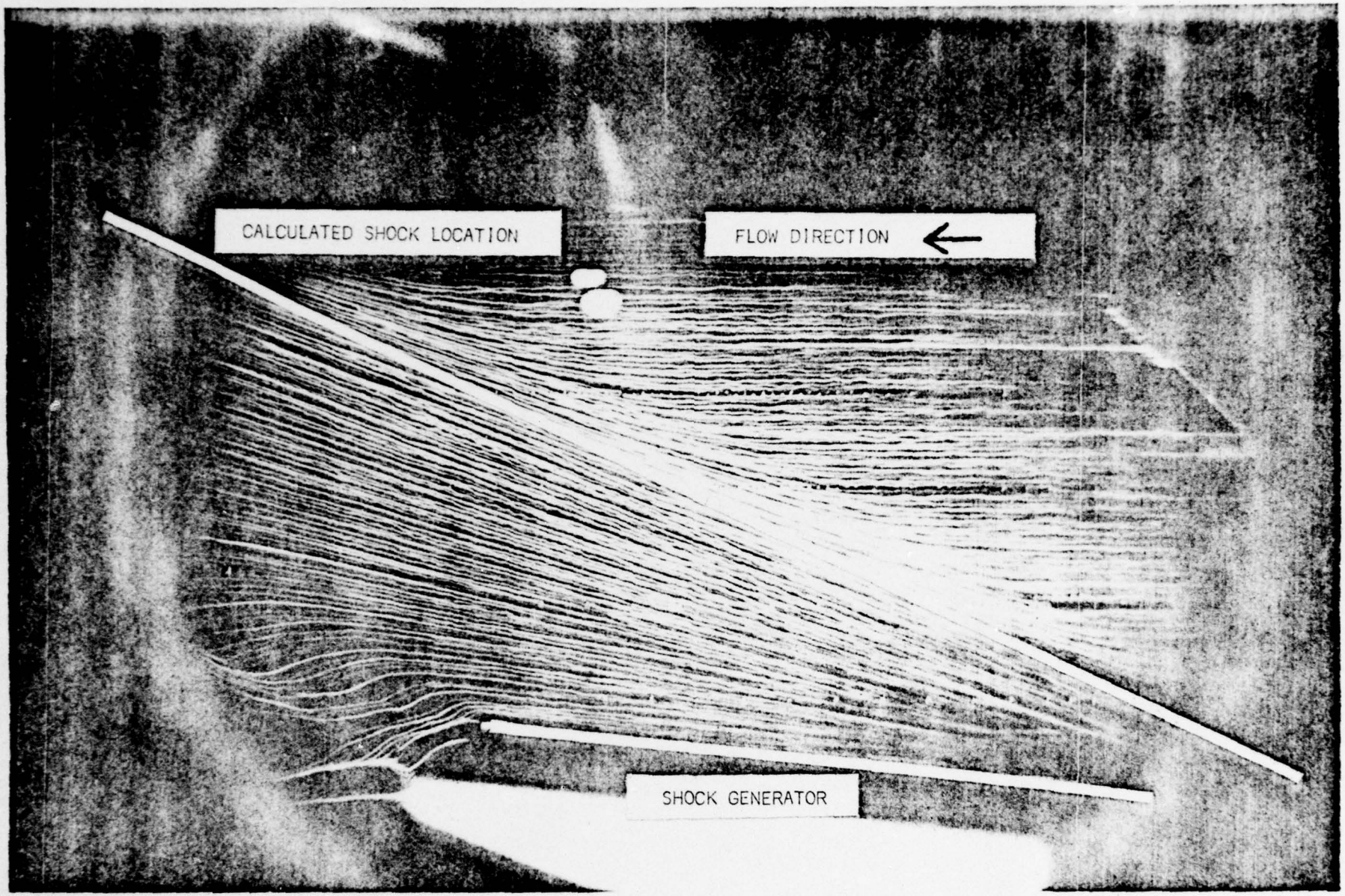

Figure 17 Surface Oil Flow Patterns $\alpha_G = 6°$

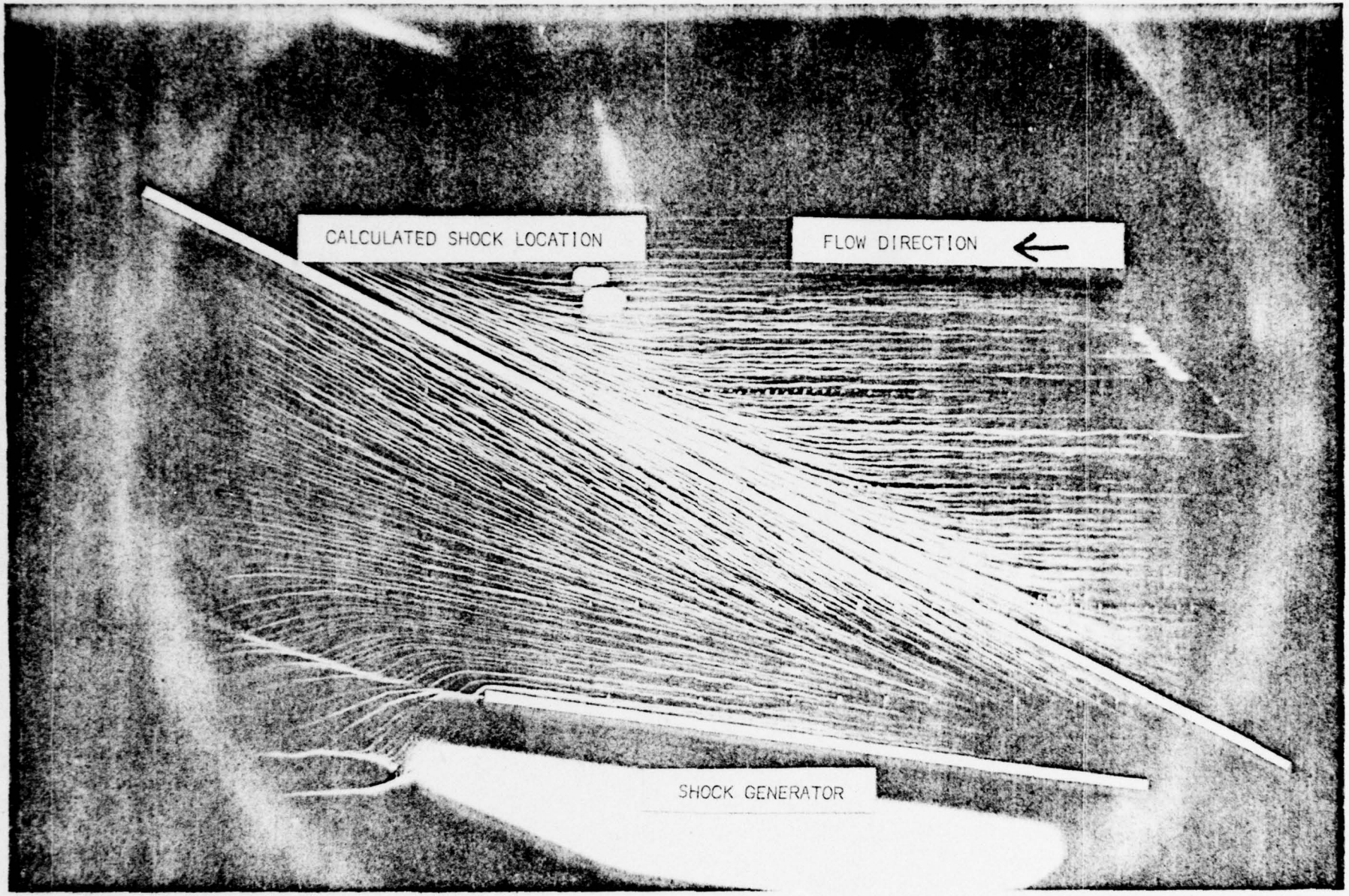

Figure 18 Surface Oil Flow Patterns $\alpha_G = 8°$

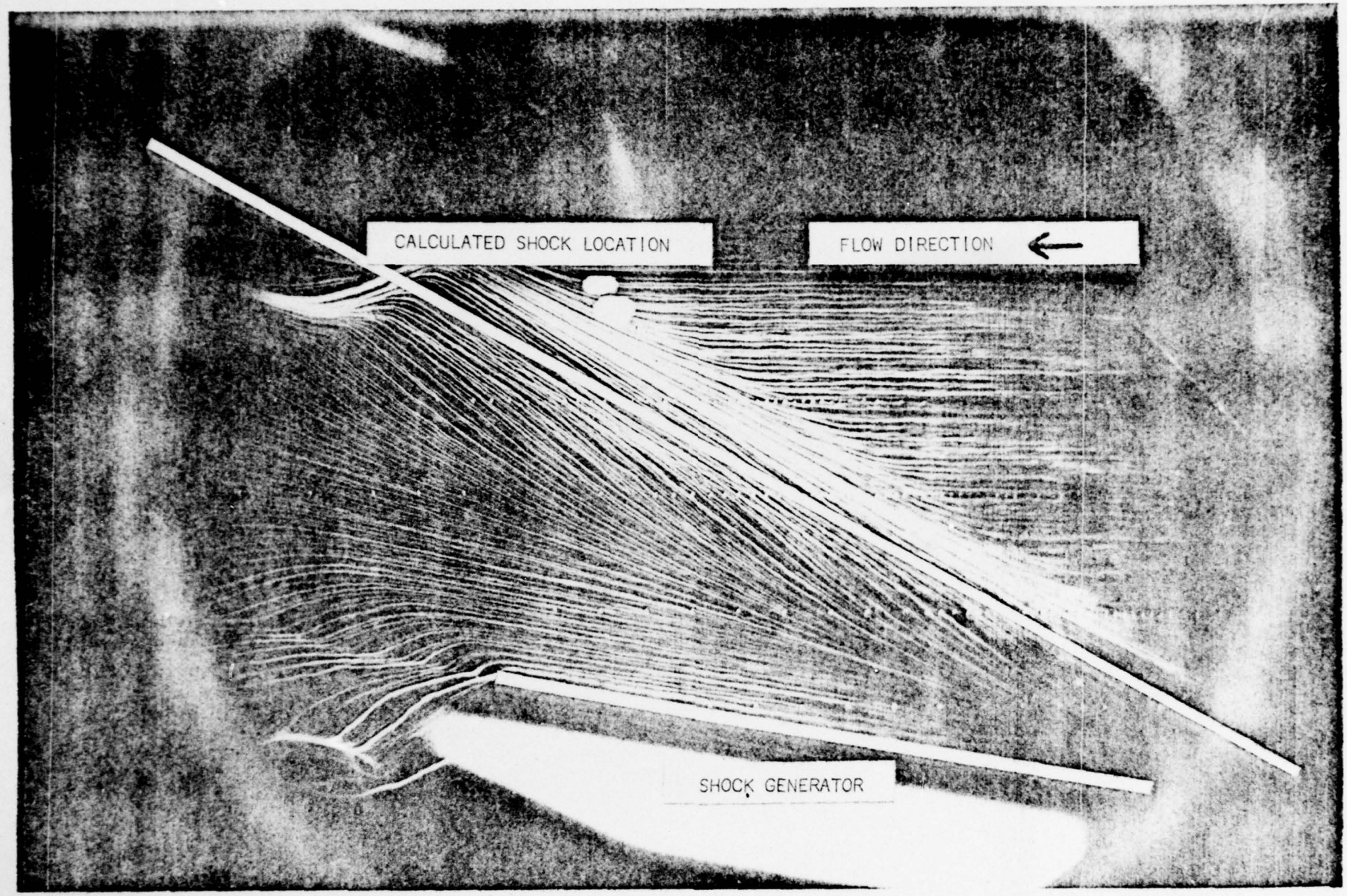

Figure 19 Surface Oil Flow Patterns $\alpha_G = 10°$

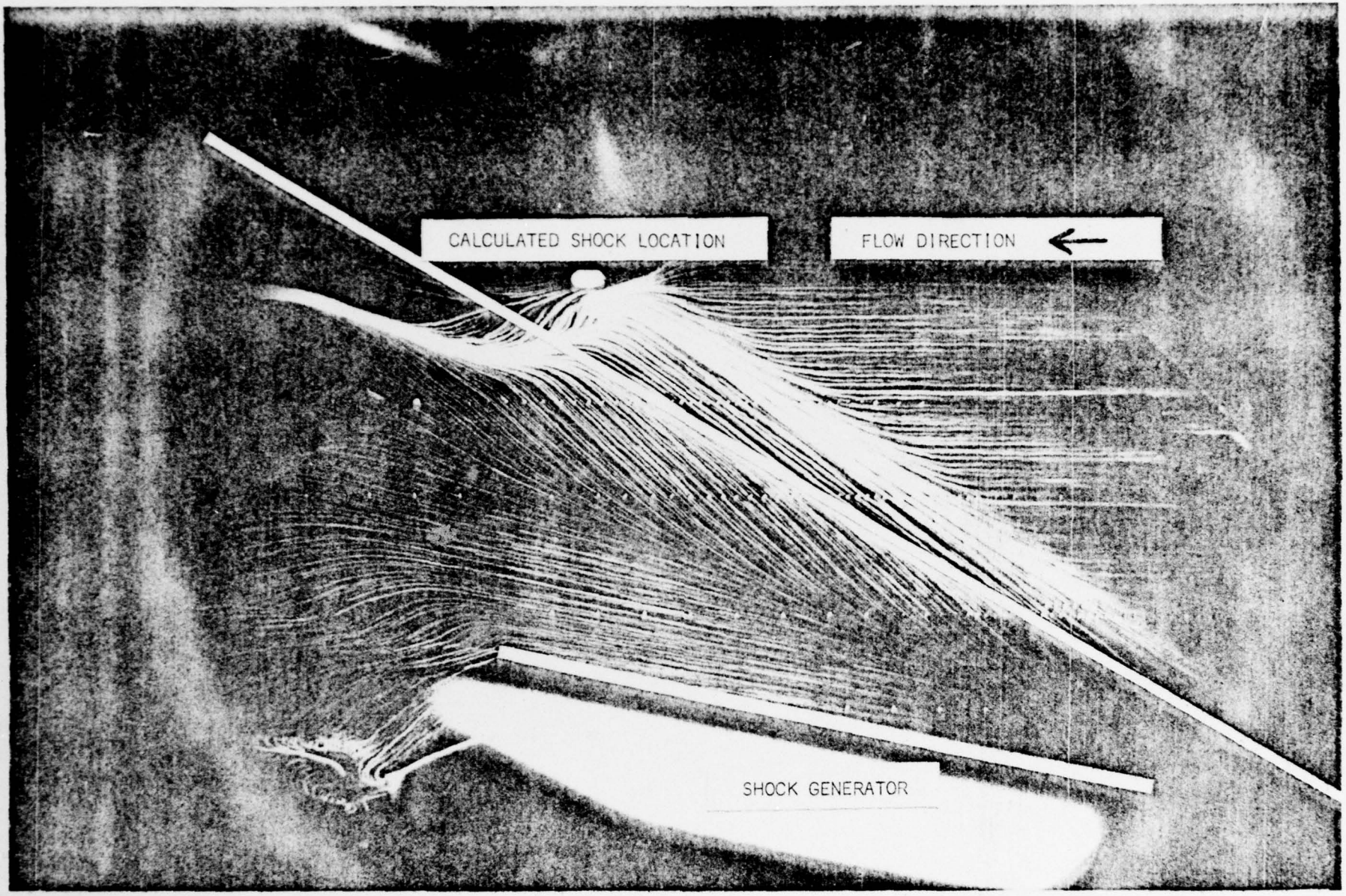

Figure 20 Surface Oil Flow Patterns $\alpha_G = 12°$

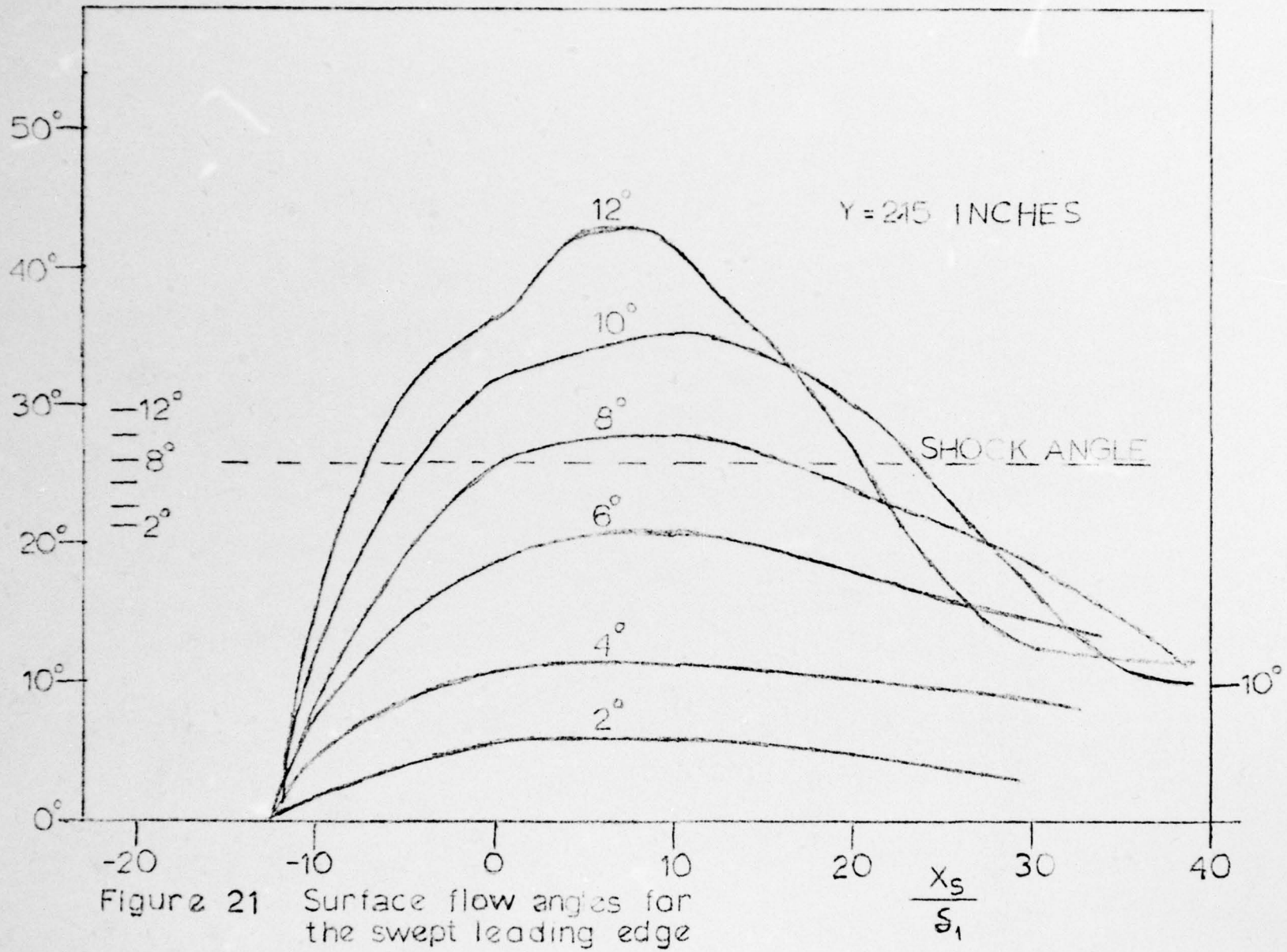

Figure 21 Surface flow angles for the swept leading edge

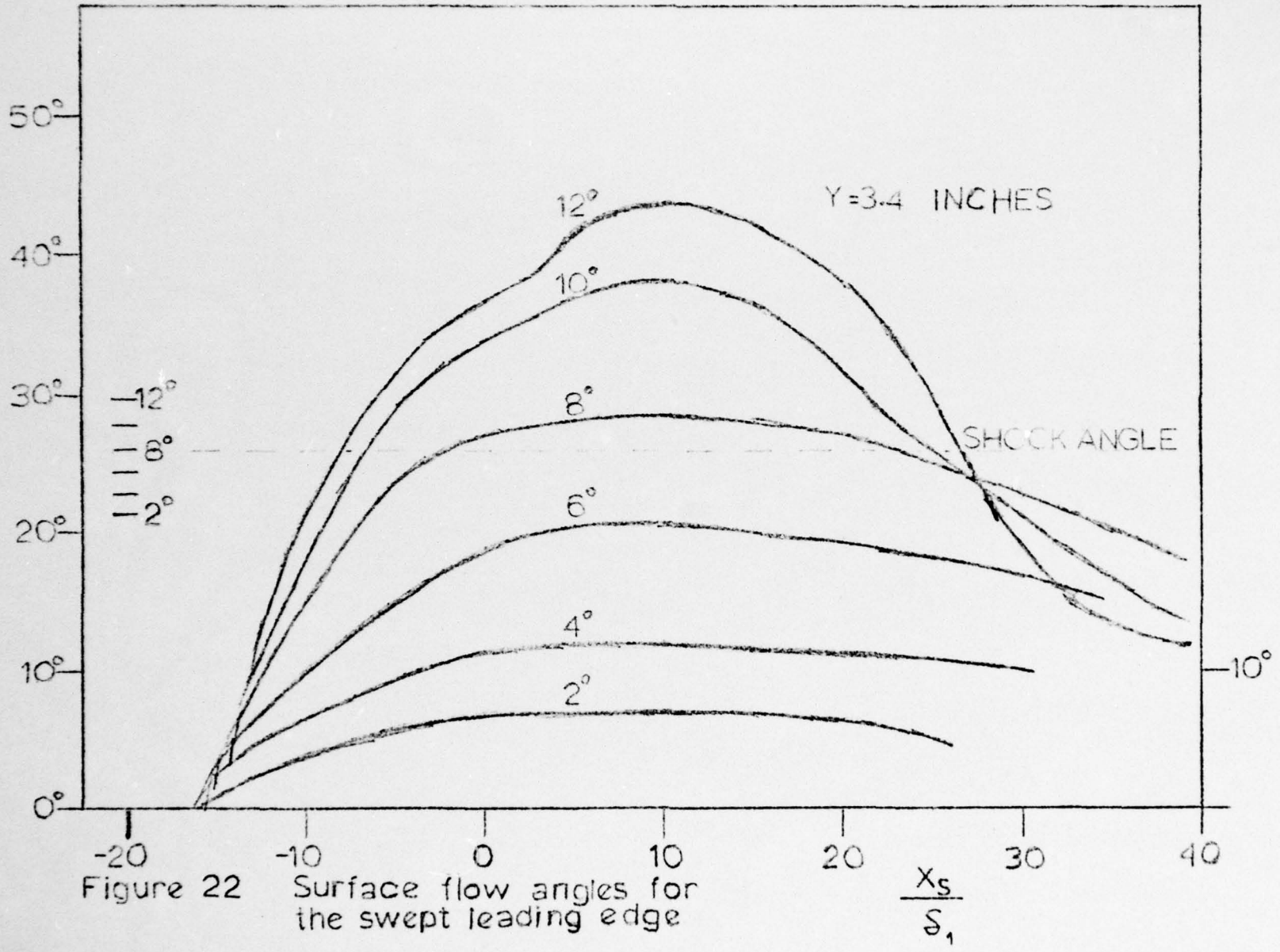

Figure 22 Surface flow angles for the swept leading edge

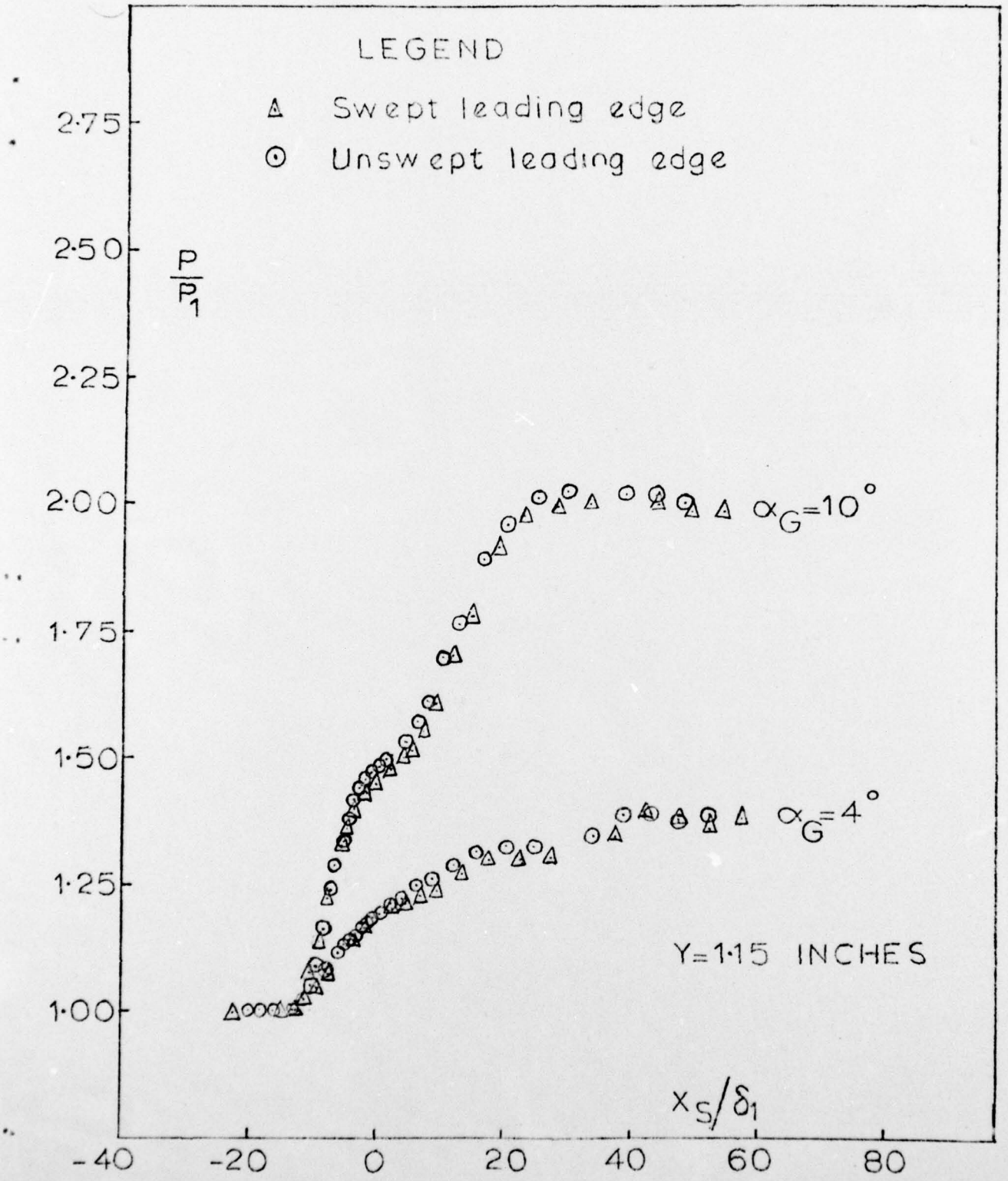

Figure 23 Comparison of surface pressure distributions on the swept and unswept leading edge models.

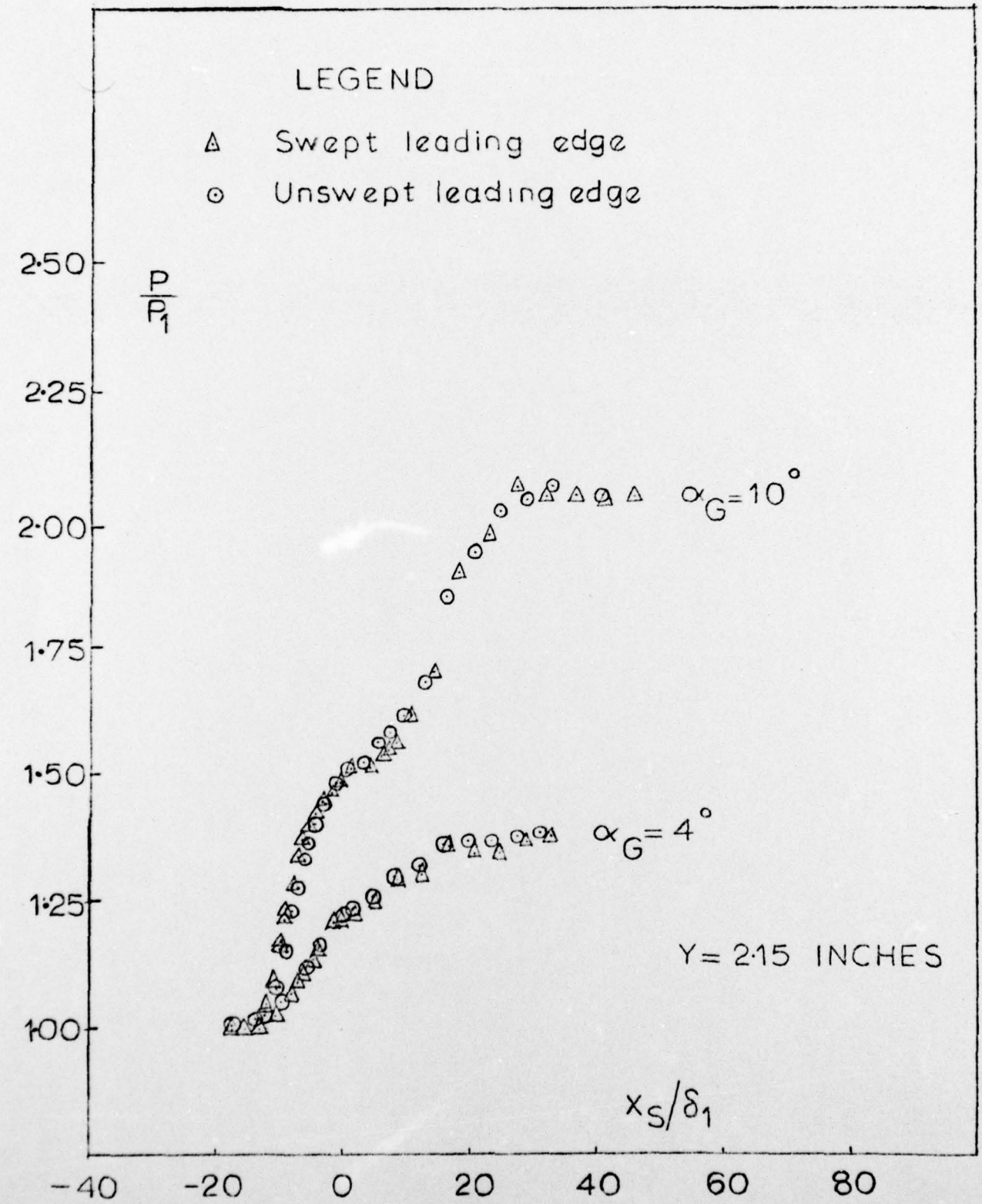

Figure 24 Comparison of surface pressure distributions on the swept and unswept leading edge models

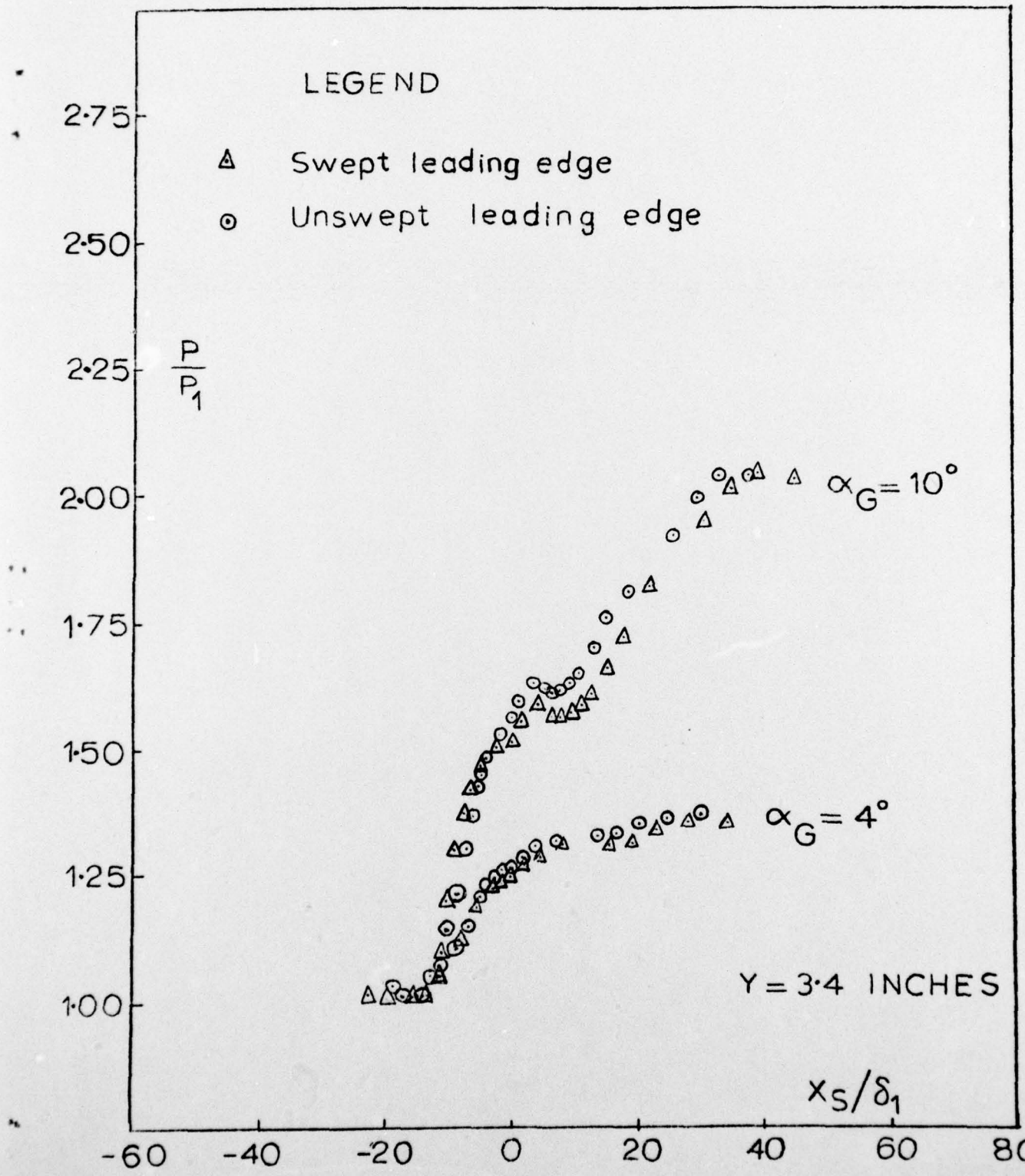

Figure 25 Comparison of surface pressure distributions on the swept and unswept leading edge models

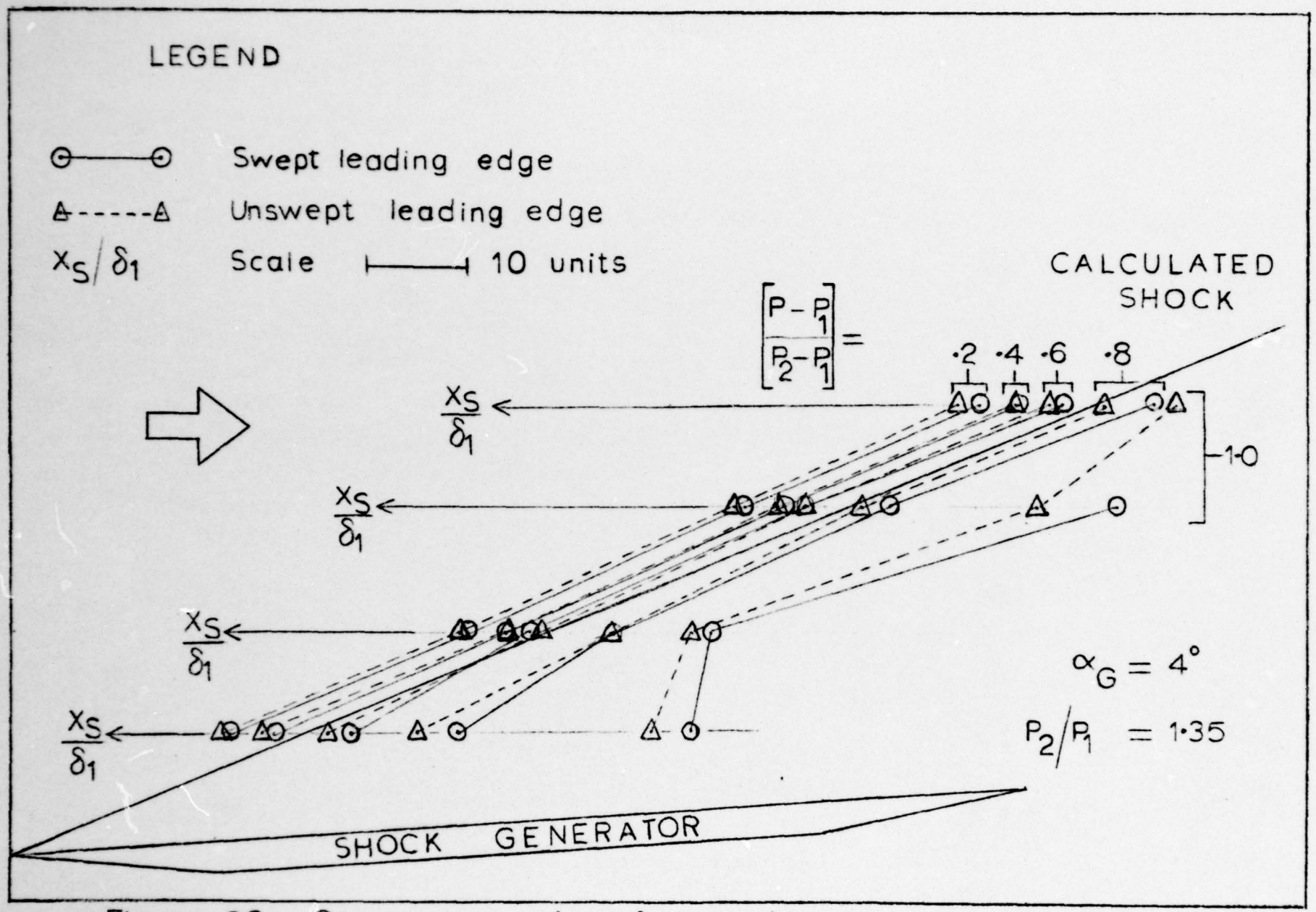

Figure 26 Comparison of surface isobar patterns for the swept and unswept leading edge models — $\alpha_G = 4°$

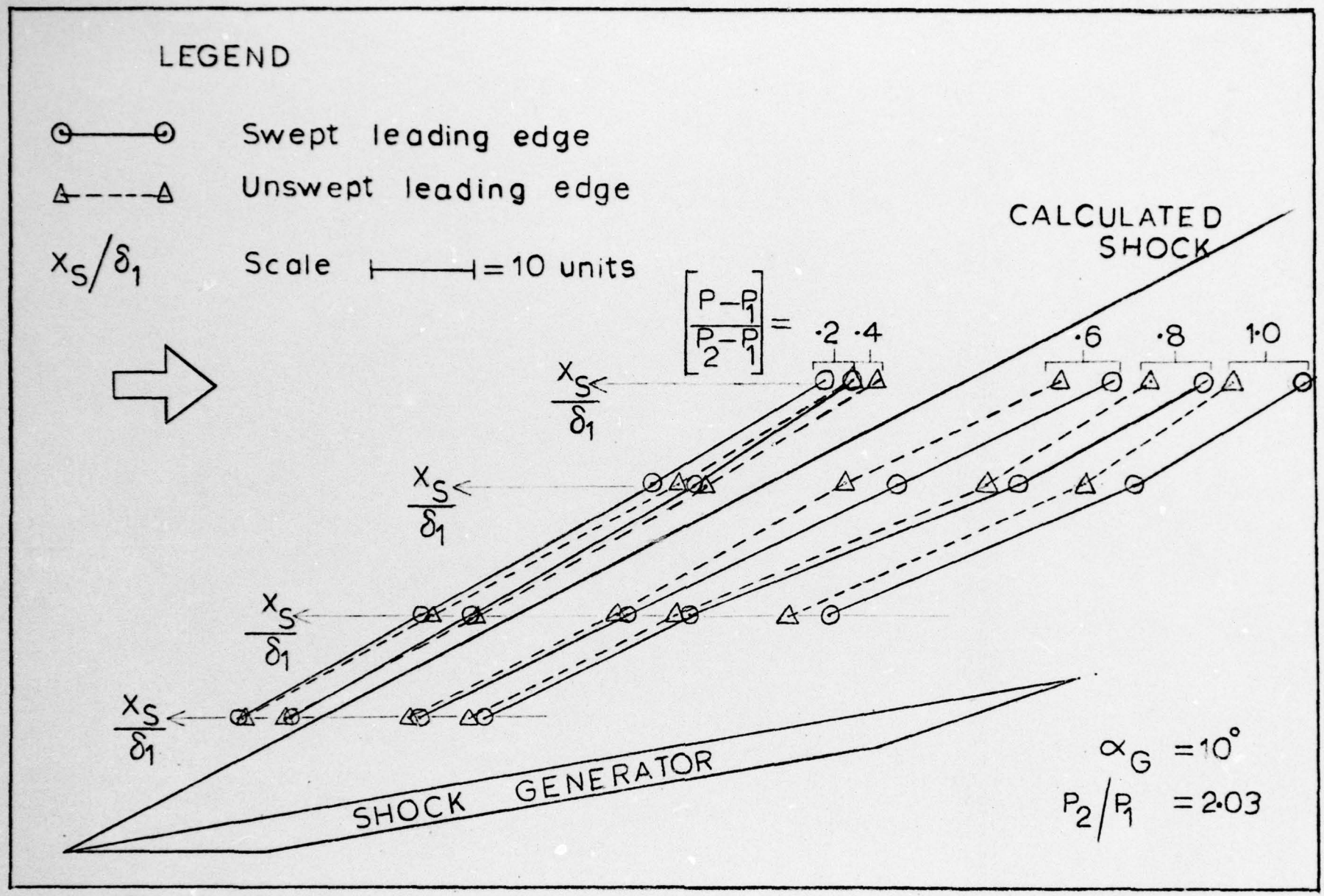

Figure 27 Comparison of surface isobar patterns for the swept and unswept leading edge models — $\alpha_G = 10°$

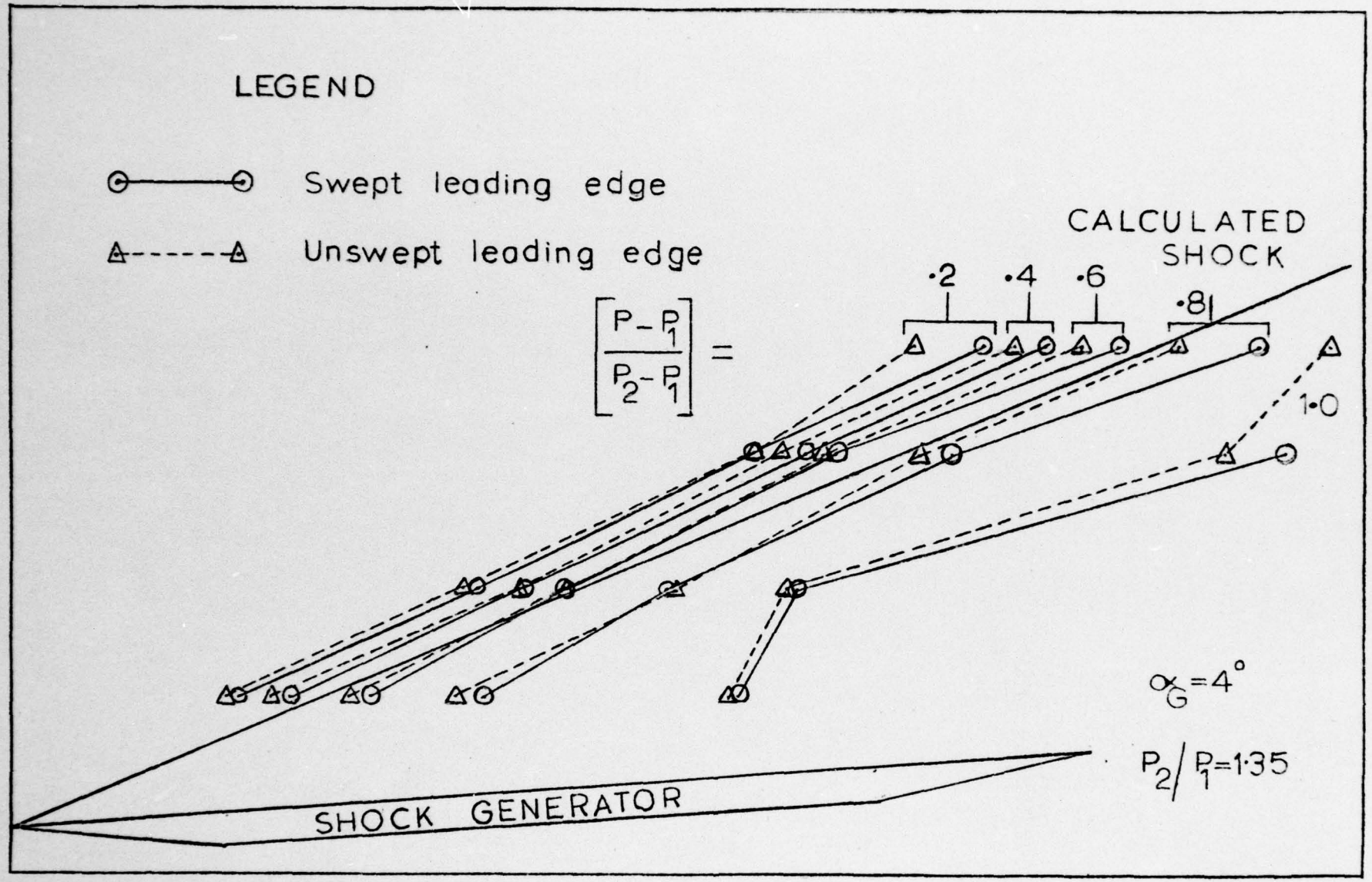

Figure 28 Comparison of surface isobar patterns for the swept and unswept leading edge models

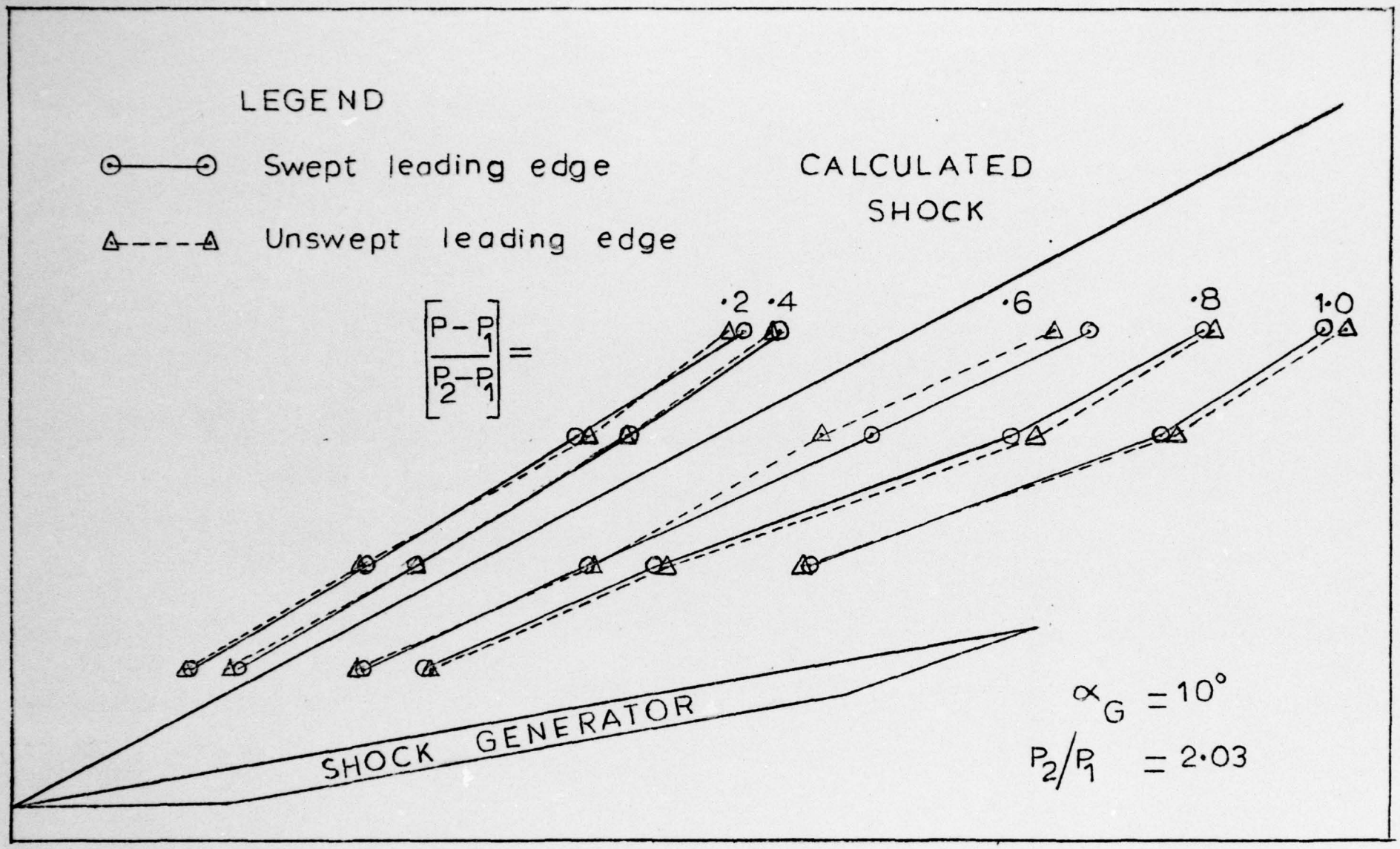

Figure 29 Comparison of surface isobar patterns for the swept and unswept leading edge models

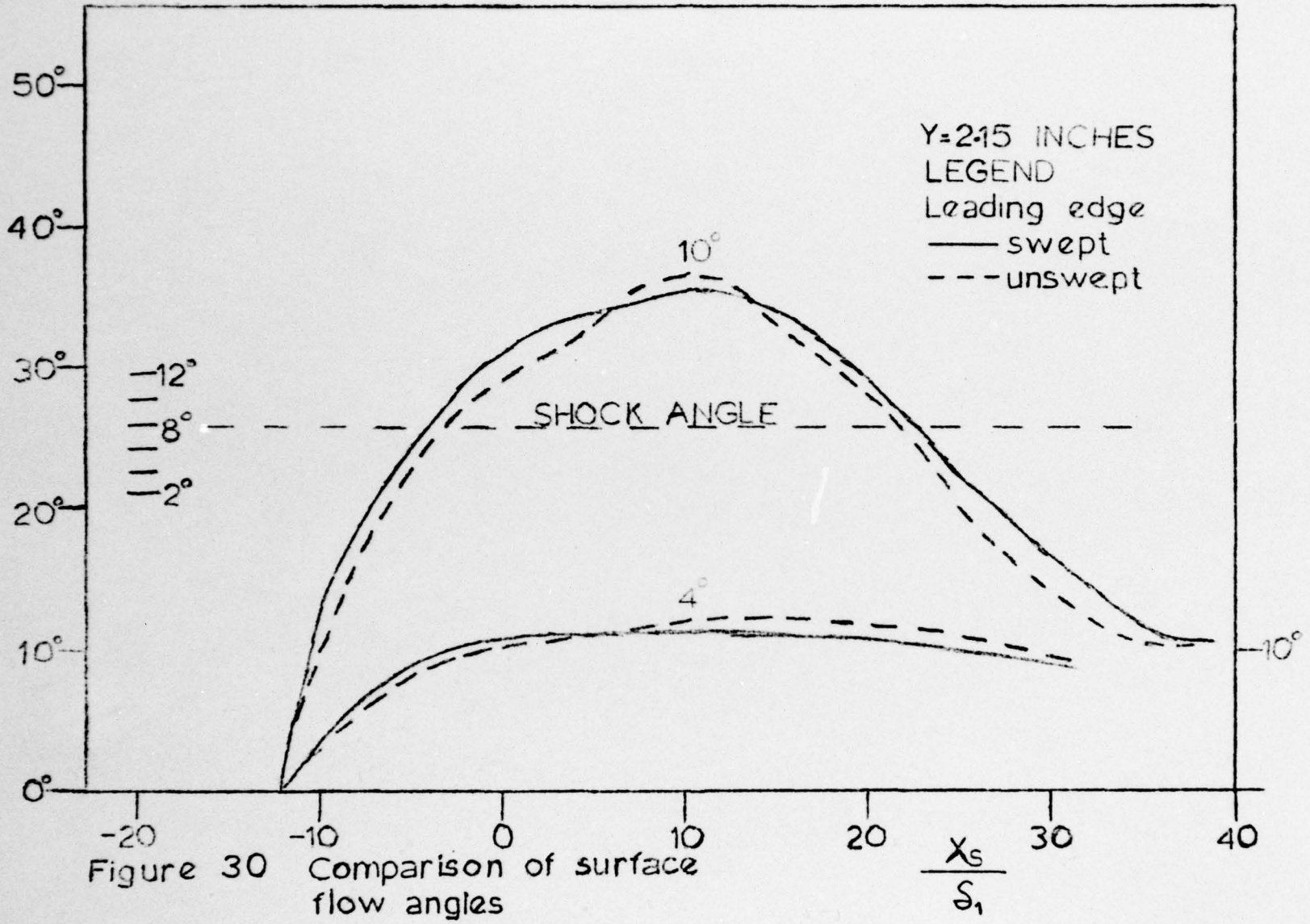

Figure 30 Comparison of surface flow angles

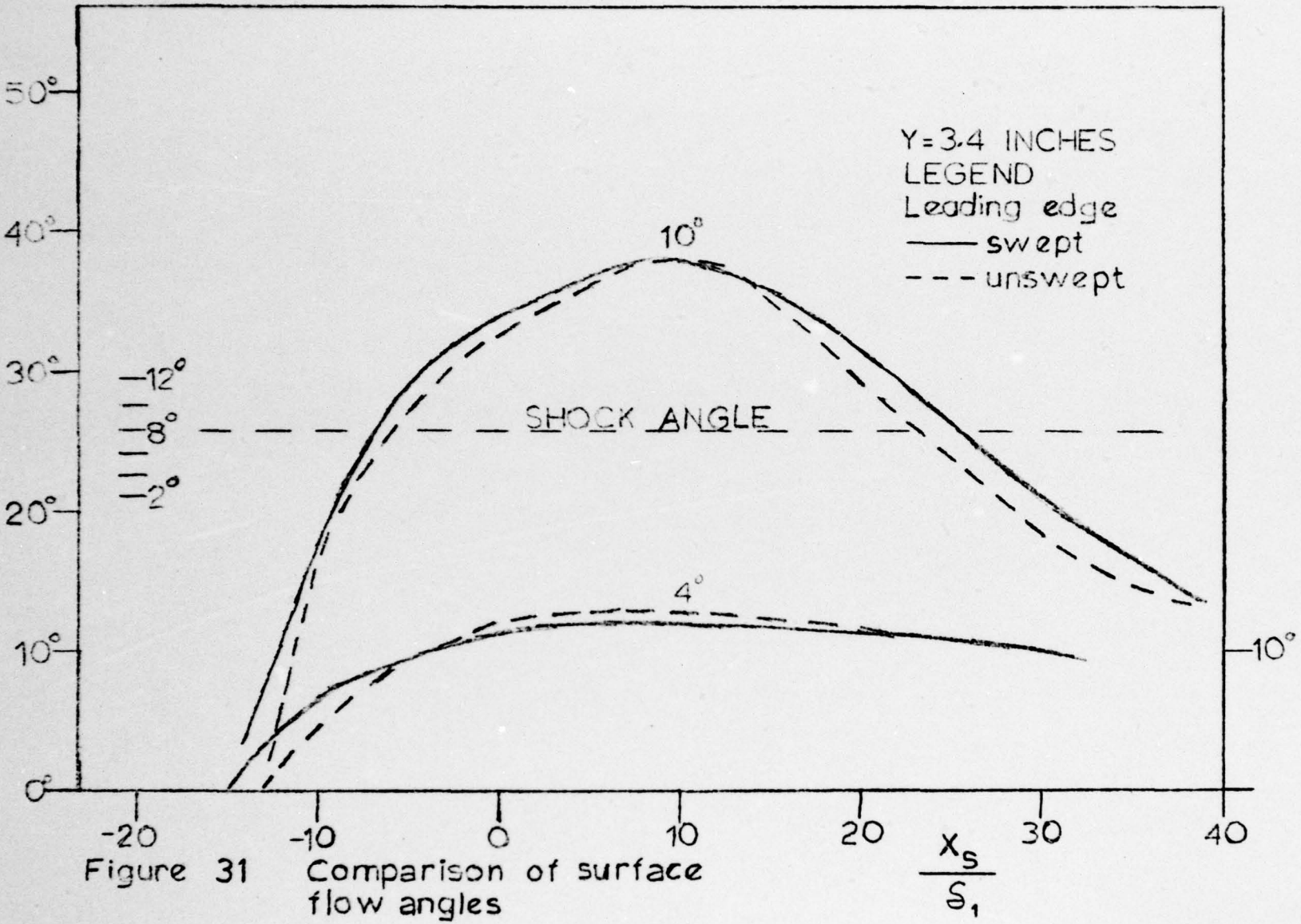

Figure 31 Comparison of surface flow angles

Unclassified
SECURITY CLASSIFICATION OF THIS PAGE (When Data Entered)

ARO 14026.1-EX

REPORT DOCUMENTATION PAGE

READ INSTRUCTIONS BEFORE COMPLETING FORM

1. REPORT NUMBER: 14026.1-EX
2. GOVT ACCESSION NO.:
3. RECIPIENT'S CATALOG NUMBER:

4. TITLE (and Subtitle): A Three-Dimensional Study of Fin-Induced Shock Wave Turbulent Boundary Layer Interaction
5. TYPE OF REPORT & PERIOD COVERED: Technical Report
6. PERFORMING ORG. REPORT NUMBER:

7. AUTHOR(s): D. S. Dolling, I. E. Vas, C. D. Cosad, S. M. Bogdonoff
8. CONTRACT OR GRANT NUMBER(s): DAAG29 76 G 0269

9. PERFORMING ORGANIZATION NAME AND ADDRESS:
Princeton University
Department of Aerospace & Mechanical Sciences
Princeton, New Jersey 08540
10. PROGRAM ELEMENT, PROJECT, TASK AREA & WORK UNIT NUMBERS:

11. CONTROLLING OFFICE NAME AND ADDRESS:
U. S. Army Research Office
Post Office Box 12211
Research Triangle Park, NC 27709
12. REPORT DATE: Jul 77
13. NUMBER OF PAGES: 44

14. MONITORING AGENCY NAME & ADDRESS(if different from Controlling Office):
15. SECURITY CLASS. (of this report): Unclassified
15a. DECLASSIFICATION/DOWNGRADING SCHEDULE:

16. DISTRIBUTION STATEMENT (of this Report)

Approved for public release; distribution unlimited.

17. DISTRIBUTION STATEMENT (of the abstract entered in Block 20, if different from Report)

18. SUPPLEMENTARY NOTES

The findings in this report are not to be construed as an official Department of the Army position, unless so designated by other authorized documents.

19. KEY WORDS (Continue on reverse side if necessary and identify by block number)

Turbulent Boundary Layers
Shock waves
Surface pressure
Flow fields
Interactions
Heat transfer

20. ABSTRACT (Continue on reverse side if necessary and identify by block number)

Surface pressure distributions and oil streak patterns have been measured in the three-dimensional flowfiled caused by the interaction of a skewed shock wave with a two-dimensional turbulent boundary layer. The boundary layer was developing on a 45° sweptback, sharp leading edged plate. Tests were made at a freestream Mach number of 2.95, a freestream unit Reynolds number of 6.3×10^7 m^{-1} (1.6×10^6 in^{-1}), a stagnation temperature of about 265°K and at near adiabatic wall temperature. Measurements have been made for generator angles in the range 0° to 12° in 2°

DD FORM 1 JAN 73 1473 EDITION OF 1 NOV 65 IS OBSOLETE

Unclassified
SECURITY CLASSIFICATION OF THIS PAGE (When Data Entered)

20. ABSTRACT CONTINUED

increments. These measurements represent the first phase of a study which will include heat transfer measurements and details of the flowfield. The measured data are presented and compared with data obtained under the same shock wave conditions but with a different boundary layer.